Research Square

Preprints are preliminary reports that have not undergone peer review.
They should not be considered conclusive, used to inform clinical practice,
or referenced by the media as validated information.

Extended JAZ degron sequence for plant hormone binding in jasmonate co-receptor of tomato SlCOI1-SlJAZ

Minoru Ueda (minoru.ueda.d2@tohoku.ac.jp)
Tohoku University
Rina Saito
Tohoku University
Kengo Hayashi
Tohoku University
Haruna Nomoto
Tohoku University
Misuzu Nakayama
Tohoku University
Yousuke Takaoka
Tohoku University
Hiroaki Saito
Hokuriku University
Toshiya Muto
Tohoku University
Souhei Yamagami
Tohoku University

Research Article

Keywords: JA-Ile, SlJAZ-SlCOI1, COI1-JAZ, plant development, reproduction, defense

Posted Date: April 12th, 2021

DOI: https://doi.org/10.21203/rs.3.rs-403224/v1

License: This work is licensed under a Creative Commons Attribution 4.0 International License.
Read Full License

Extended JAZ degron sequence for plant hormone binding in jasmonate co-receptor of tomato *Sl*COI1-*Sl*JAZ

Authors:

Rina Saito[1], Kengo Hayashi [2], Haruna Nomoto[2], Misuzu Nakayama[2], Yousuke Takaoka [2], Hiroaki Saito [3], Souhei Yamagami[1], Toshiya Muto[2], and Minoru Ueda*[1,2]

Affiliations:

[1]Department of Molecular and Chemical Life Sciences, Graduate School of Life Sciences, Tohoku University, Sendai 980-8578, Japan

[2]Department of Chemistry, Graduate School of Science, Tohoku University, Sendai 980-8578, Japan

[3] Center for Basic Education, Faculty of Pharmaceutical Sciences, Hokuriku University, Kanazawa, 920-1181, Japan

*Correspondence: minoru.ueda.d2@tohoku.ac.jp

Abstract

(+)-7-*iso*-jasmonoyl-L-isoleucine (JA-Ile) is a lipid-derived phytohormone implicated in plant development, reproduction, and defense in response to pathogens and herbivorous insects. All these effects are instigated by the perception of JA-Ile by the COI1-JAZ co-receptor in the plant body, which in *Arabidopsis thaliana*, is profoundly influenced by the short JAZ degron sequence (V/L)P(Q/I)AR(R/K) of the JAZ protein.

Here, we report that *Sl*JAZ-*Sl*COI1, the COI1-JAZ co-receptor found in the tomato plant, relies on the extended JAZ degron sequence (V/L)P(Q/I)AR(R/K)XSLX instead of the canonical JAZ degron. This finding illuminates our understanding of the mechanism of JA-Ile perception in this plant, and will inform the genetic modification of the *Sl*COI1-*Sl*JAZ co-receptor to improve JA-Ile perception and the development of the synthetic agonists / antagonists.

Lipid-derived (+)-7-*iso*-jasmonoyl-L-isoleucine (JA-Ile) is a major class of phytohormones implicated in plant development, reproduction, and the defense response of plants against pathogens and herbivorous insects.[1,2] Exposure of plants to external stress causes jasmonate signaling, which is triggered by the production of JA-Ile from jasmonic acid (JA).[3,4] Perception of JA-Ile by the COI1-JAZ co-receptor cause upregulation of of JA-responsive genes, leading to the expression of JAZ (JASMONATE ZIM-DOMAIN) repressor protein –a hub of jasmonate signaling.[5,6]

The JAZ protein contains two major functional domains: Jas and TIFY. In the absence of JA-Ile, the Jas domain causes JAZ to interact with various transcription factors (TFs), including the master regulator MYC2.[7] The ethylene-responsive element binding factor-associated amphiphilic repression (EAR) domain in TIFY is a binding site for Novel Interactor of JAZ (NINJA) and recruits co-repressor TOPLESS (TPL) through NINJA.[8] Through these interactions, JAZ constructs a transcriptional repression machinery consisting of the MYC2-JAZ-NINJA-TPL complex, which repress the expression of JA-responsive gene. In the presence of JA-Ile, JAZ also plays an important role in releasing the repression of TFs. The Jas motif is also important for protein-protein interaction with COI1, a subunit of SCF^{COI1}E3 ubiquitin ligase, to form COI1-JA-Ile-JAZ co-receptor complex for JA-Ile ligand.[9] JA-Ile cause COI1-JAZ co-receptor formation and subsequent ubiquitination and degradation of JAZ to derepress the expression of JA-responsive genes.[10-12]

Recently, it has become clear that *JAZ* genes function redundantly; however, each *JAZ* subfamily gene is also responsible for its own unique function,[13-17] and differences in the sequence of the Jas motif profoundly influence the unique function of each JAZ. This is in part because the function of JAZ depends on how strongly and with which of the many TFs it interacts.[13] The Jas motif also affects the lifespan of each JAZ in plant cells (through the affinity between JAZ and COI1) which in turn determines the duration of effect of each JAZ's unique function.[13]

The crystal structure of the COI1-JA-Ile-JAZ1 degron peptide revealed that the short JAZ degron sequence in the Jas motif is responsible for COI1-JA-Ile-JAZ1 complex formation based on the discovery of a hydrogen bond-network between the JAZ1 degron sequence LPIARR and the COI1-JA-Ile complex.[18] JAZ belongs to the TIFY protein family, but only the JAZ subfamily incorporates the Jas motif, including short canonical

degron sequence LPIAR(R/K) necessary to trap JA-Ile (**Figure 1a&1b**). The JAZ degron sequence is highly conserved among plant species, except for the two non-canonical degron sequences IPMQRK of *Fa*JAZs found in the strawberry plant *Fragaris X ananassa*, and MPIARK of *Ec*JAZ1 found in finger millet *Eleusine coracana* (L.) Gaertn.[19-21]

Small differences in the *Arabidopsis* JAZ degron sequences (identity 37.0% in **Figure 1a**) are considered to account for the difference in affinity (K_D) between JAZ and COI1-JA-Ile.[22] However, the 12 JAZs of *Solanum lycopersicum* have a remarkably well-conserved JAZ degron sequence (V/L)P(Q/I)AR(R/K) (identity 46.6% in **Figure 1a**), suggesting their affinities (K_D) for the *Sl*COI1-JA-Ile complex are very similar (**Figure 1a**). Here, we report the first comprehensive study of the affinity of the *Sl*JAZ-*Sl*COI1 co-receptor for JA-Ile, and demonstrate that the perception of JA-Ile depends on the extended JAZ degron sequence (V/L)P(Q/I)AR(R/K)XSLX. This use of an extended degron sequence (instead of the canonical short JAZ degron sequence) accounts for the different affinities of *Sl*JAZ and *Sl*COI1-JA-Ile.

Results

The affinities of *Sl*JAZ1-11/13 for *Sl*COI1-JA-Ile are different

All the *TIFY* sequences of the JAZ proteins of *Solanum lycopersicum* have been previously reported: 19 *TIFY* genes including 12 canonical *JAZ* (*Sl*JAZ1-11/13) and non-canonical *SlJAZ12* genes are encoded in the *Solanum lycopersicum* genome.[23-25] The Jas motifs of the 12 canonical *SlJAZs* are remarkably similar to the *Arabidopsis* consensus Jas motif $SLX_2FX_2KRX_2RX_5PY$, and the JAZ degron sequence (V/L)P(Q/I)AR(R/K) wherein the hydrophobic L/V is conjugated with P(Q/I)AR and followed by basic R/K is conserved in 8 out of 12 *SlJAZs* (*Sl*JAZ1-6/8/13) (**Figures 1a & 1b**). Accordingly, *Sl*COI1-*Sl*JAZ1-6/8/13 are expected to perceive JA-Ile with equal affinity, whereas *Sl*COI1-*Sl*JAZ9-11 (which incorporate a non-canonical JAZ degron) are not expected to perceive it at all. Accordingly, we examined the affinities of 12 *Sl*JAZ proteins for the *Sl*COI1-JA-Ile complex by pull-down assay.

SlJAZ genes were cloned from the tomato cultivar Micro-Tom and their FLAG-tag-fused proteins FLAG-*Sl*JAZ1-11/13 expressed using the wheat germ-derived cell-free

protein expression system (**Figure S1**). The protein GST-fused *Sl*COI1 (GST-*Sl*COI1) was also expressed in Sf9 cultured insect cells (**Figure S2**). *Arabidopsis* ASK protein was co-expressed to improve the stability of *Sl*COI1.[26] As expected, SlJAZ1-3/5-8 but not FLAG-*Sl*JAZ9-11 pull-down the GST-*Sl*COI1 in the presence of 100 nM JA-Ile (**Figure 2a**). However, *Sl*JAZ4/13 (which incorporates the same canonical JAZ degron LPIARR as *Sl*JAZ1-3) could not pull-down the GST-*Sl*COI1 under the same condition (**Figures 1b and 2a**). Identical results were obtained using coronatine (COR), a naturally occurring phytotoxin known as structural mimic of JA-Ile, in place of JA-Ile, suggesting that COR is perceived by the co-receptor in a similar manner to JA-Ile (**Figure S3**). These results indicate that sequences other than the highly conserved *Sl*JAZ degron in full-length JAZ affect the perception of JA-Ile by the *Sl*COI1-*Sl*JAZ co-receptor.

To examine the effect of the exo-degron sequence quantitatively, we designed and synthesized fluorescein-tagged *Sl*JAZ1-11/13 degron short peptides (*Sl*JAZP1-11/13) of 27 amino acids (**Figure 3a** and **Figure S4** -**S5**) based on previous work on *Arabidopsis* COI1-JAZ.[22] The pull-down assay using the GST-*Sl*COI1 and Fl-*Sl*JAZ degron peptides in the presence of increasing concentrations of JA-Ile yielded very similar results to those obtained using full-length *Sl*JAZs (**Figures 2b-d**). Therefore, the affinity of full-length JAZ was confirmed to depend on the sequence in these short peptides. The observed affinities were quantitatively assessed in AlphaScreen luminescence proximity assays using *Sl*JAZPs and GST-*Sl*COI1 in the presence of 0-30 μM JA-Ile (**Figure 3b and Figure S6**),[7,27] and found to be in good accordance with the results obtained by pull-down assay: 20>K_d for *Sl*JAZ1/5-8 of strong affinity, 150>K_d for *Sl*JAZ2/3 of weak affinity, K_d> 400 for *Sl*JAZ4/9-11/13 of no/little affinity (**Table 1**). Similar results were obtained using COR (**Figures S7** and **S8**).

Hormone perception relies on extended JAZ degron sequences in tomato *Sl*JAZs

Here we focused on the relationship between the degron sequences of *Sl*JAZPs and their K_d values. The short JAZ degron sequence (L/V)P(Q/I)AR(R/K) was highly conserved in *Sl*JAZP1-6/8/13 (**Figure 3a**). *Sl*JAZP5/6/8, which incorporate the JAZ degron sequence VPQARK all have strong affinity for *Sl*COI1-JA-Ile. In contrast,

126 remarkable differences in affinity was observed for *Sl*JAZP1-4/13, whose degron
127 sequence is LPIARR: only *Sl*JAZP1 showed moderate affinity for *Sl*COI1-JA-Ile; the
128 others had weak/no affinity. Among SlJAZ1-4/13, the difference can be found in
129 downstream-of-degron (DOD) sequence XSLX (**Figure 3a**). This strongly suggests that
130 sequences longer than the canonical JAZ degron influence the affinity of *Sl*JAZs for
131 *Sl*COI1-JA-Ile.

132 To confirm the effect of exo-JAZ-degron sequence within *Sl*JAZPs on their
133 affinity, we prepared chimeric *Sl*JAZPs of swapped sequence and submitted them to the
134 AlphaScreen assay. First, we swapped the two JAZ-degron sequences VPQARK of
135 *Sl*JAZP5/6/8 and LPIARR of *Sl*JAZP1-4/13 to examine the effect of JAZ degron
136 sequence for the difference in affinity. The *N*-terminal region of high-affinity peptide
137 *Sl*JAZP5 including JAZ-degron VPQARK was swapped with that of moderate/little-
138 affinity *Sl*JAZP1/4 including JAZ-degron LPIARR to provide the swapped peptide
139 *Sl*JAZP1/4-5 (**Figures 4a, S9 and S10**). Then, we examined whether the difference in
140 JAZ degron sequence of *Sl*JAZs affect the affinity with *Sl*COI1-JA-Ile (**Figure 4ab**, and
141 S11). As shown in Figure 4b, high affinity of *Sl*JAZP5 was moderately decreased by
142 swapping with *Sl*JAZP1/4 (K_d = 4.2 nM for *Sl*JAZP5 to K_d = 16.5 nM for *Sl*JAZP1/4-5).
143 The effect of swapping was moderate and the complete swapping of their affinities did
144 not occur. This result suggested that the differences in JAZ degron alone cannot fully
145 account for the difference in their affinities, which must therefore be influenced by exo-
146 JAZ-degron sequences in addition to the canonical JAZ degron.

147 To examine the effect of DOD sequence, we studied *Sl*JAZP1-4/13 which
148 incorporate the same JAZ degron sequence LPIARR and alternative DOD sequence
149 XSLX. We focused on three SlJAZPs, *Sl*JAZP1 of strong affinity (K_d = 9.2 nM), *Sl*JAZP3
150 of moderate affinity (K_d = 136 nM), and *Sl*JAZP4 of no affinity (K_d = 1776 nM). We
151 prepared the *Sl*JAZP1-3DOD and *Sl*JAZP1-4DOD in which DOD sequence of *Sl*JAZP1
152 was swapped with that of *Sl*JAZP3 and *Sl*JAZP4, respectively (**Figure 4a,** and **S9–11**).
153 As shown in **Figure 5ab**, their affinities with *Sl*COI1-JA-Ile were moderately dropped by
154 this swapping (K_d = 28.4 nM for *Sl*JAZP1-3DOD and K_d = 46.9 nM for *Sl*JAZP1-4DOD).
155 This result confirmed that DOD sequence in addition to JAZ degron affects the affinity
156 between *Sl*JAZ and *Sl*COI1-JA-Ile. Next we examine whether DOD sequence also affect
157 the affinity in *Sl*JAZP5/6/8 of another JAZ degron sequence VPQARK in common. As

158 *Sl*JAZP5/6/8 have the same DOD sequence of ASLA, we replaced DOD of *Sl*JAZP5 of
159 strong affinity (K_d = 4.2 nM) to with that of *Sl*JAZ2 of weak affinity (K_d = 134 nM). We
160 prepared DOD swapped peptides *Sl*JAZP5-2DOD (ASLA of *Sl*JAZ5 to NSLT of *Sl*JAZ2)
161 and *Sl*JAZP2-5DOD (NSLT of *Sl*JAZ2 to ASLA of *Sl*JAZ5) (**Figures 4a,** and **S9–11**).
162 Their affinities with *Sl*COI1-JA-Ile were affected by this swapping (K_d = 11.7 nM for
163 *Sl*JAZP5-2DOD and K_d = 42.7 nM for *Sl*JAZP2-5DOD, **Figure 5cd**). This result
164 suggested that DOD sequence in *Sl*JAZ5/6/8 also affects the affinity with *Sl*COI1-JA-Ile.
165 Moreover, we swapped the extended JAZ degron sequence including JAZ-degron
166 and DOD to prepare the swapped peptides of *Sl*JAZP5-2 (DLPIARRNSLT of SlJAZ2
167 into AVPQARKASLA of SlJAZ5) and *Sl*JAZP2-5 (AVPQARKASLA of SlJAZ5 into
168 DLPIARRNSLT of SlJAZ2) (**Figure 4a,** and **S9–11**). Their affinity with *Sl*COI1-JA-Ile
169 was completely replaced each other by this sequence swapping (K_d = 88.8 nM for
170 *Sl*JAZP5-2 and K_d = 5.0 nM for *Sl*JAZP2-5, respectively, **Figure 5ef**). This result
171 confirmed that extended JAZ degron sequence including JAZ-degron and DOD affects
172 the affinity of in SlJAZ with *Sl*COI1-JA-Ile.
173 From all of these results, we concluded that extended-JAZ-degron sequences,
174 VPQARKASLA or LPIARRXSLX, determine the affinity of *Sl*JAZs with *Sl*COI1-JA-Ile.
175
176 ***In silico* simulation demonstrated the role of extended JAZ degron sequences**
177 **in *Sl*COI1-JA-Ile-*Sl*JAZ complex formation.**
178 *In silico* docking simulation studies using the crystal structure of *Arabidopsis*
179 COI1-JA-Ile-JAZ1 have previously enabled the study of the JA-Ile binding mode of the
180 COI1-JAZ co-receptor of other plant species, such as *Phaseolus lunatus*, *Eleusine*
181 *coracana* (L.) Gaertn, *Fragaria vesca*, and *Fragaria* × *ananassa*.[20,21,28,29] The
182 contribution of the extended JAZ degron sequence to *Sl*COI1-JAIle-*Sl*JAZ complex
183 formation was examined by comparing the crystal structure of *Arabidopsis* COI1-JAIle-
184 JAZ1 with the *in silico* interaction models of *Sl*COI1-JAIle-*Sl*JAZ1 and *Sl*COI1-JAIle-
185 *Sl*JAZ5, which have an affinity for JA-Ile. A homology model of *Sl*COI1 was obtained
186 with MOE based on the crystal structure of *At*COI1 complexed with JA-Ile and using
187 *At*JAZ1 (PDB ID: 3OGL) as a template (the sequence identity of *Sl*COI1 and *At*COI1 is
188 68.1%). Then, *At*JAZ1 was replaced with *Sl*JAZ1 or *Sl*JAZ5. The obtained models of
189 these complexes (*Sl*COI1-JAIle-*Sl*JAZ1 and *Sl*COI1-JAIle-*Sl*JAZ5) were then used for

subsequent molecular dynamics (MD) simulations. Root means square deviation (RMSD) values indicated that the structures reached equilibrium in after 50 ns or more (**Figure 6ab**). There was no significant difference in the interaction of the canonical JAZ degron sequence in JAZ/*Sl*JAZ with COI1/*Sl*COI1 and the ligand JA-Ile, or in the hydrogen-bonding network formed around JA-Ile (**Figures 6c-e, and 7a-f**) an any of the three complexes. In addition, no direct interaction between the DOD sequence of *Sl*JAZs and JA-Ile was observed in *Sl*COI1-JA-Ile-*Sl*JAZ1/5. These results suggest that the DOD sequence in *Sl*JAZs contributes to the enhancement of the interaction with *Sl*COI1. Next, we compared the interaction between the DOD sequence and *Sl*COI1 in *Sl*COI1-JAIle-*Sl*JAZ1/5 with the interaction between the corresponding sequence in JAZ1 (ASLH) and COI1. In COI1-JAIle-JAZ1, weak interaction through one hydrogen bond was found between the DOD sequence and COI1, whereas in *Sl*COI1-JAIle-*Sl*JAZ1 and *Sl*COI1-JAIle-*Sl*JAZ5, strong interaction by several hydrogen bonds or hydrophobic interactions were found (**Figure 7bc and hi**). This indicates that the DOD sequence in *Sl*JAZ significantly contributes to the formation of the *Sl*COI1-JAIle-*Sl*JAZ complex, in support of the results of the wet experiments.

Discussion

JAZ functions as a repressor of numerous TFs in plant cells, and the differences in function between JAZ family proteins are profoundly affected by how strongly and with which of the many TFs each JAZ interacts. Since JAZs interact with many TFs through the Jas motif, differences in this motif can account for differences in the function of JAZs. In addition, JAZ interacts with the COI1-JA-Ile complex using the degron sequence within the Jas motif and ubiquitinated and degraded as a substrate for E3 ubiquitin ligase. A small difference in the degron sequence of each JAZ can profoundly impact the duration of JAZ function because it affects the lifetime of each JAZ in the plant cell. Therefore, differences in the strength of the interaction between each JAZ and the COI1-JA-Ile complex affect the function of each JAZ. [30]

This study is the first comprehensive investigation into the affinity of the *Sl*JAZ-*Sl*COI1 co-receptor for JA-Ile. Surprisingly, *Sl*JAZ9-11 were found to have no affinity for *Sl*COI1-JA-Ile, despite having a canonical JAZ degron sequence. In transcript expression

of *Sl*JAZs on JA-treated Micro-Tom, *Sl*JAZ9-11 are also JA-responsive: *Sl*JAZ9/10 are weakly induced in both roots and leaves, and *Sl*JAZ11 is strongly induced in roots but weakly in leaves.[23] In the case of *Arabidopsis*, non-canonical JAZ7/8/13 lacking a conserved degron sequence do not have affinity for COI1-JA-Ile and play a unique role in transcriptional repression in plant cells.[31,32] JAZ10.4, an alternative splice variant of JAZ10, is involved in the negative feedback regulation of JA signaling and is responsible for the delayed repression of activated JA signals.[33] A similar function is inferred for JA-responsive *Sl*JA9-11, despite its lack of affinity for SlCOI1-JA-Ile.

The crystal structure of *Arabidopsis* COI1-JA-Ile-JAZ1 complex revealed important details regarding the interaction between JAZ and COI1-JA-Ile complex. The short canonical degron sequence LPIARR of JAZ1 overlies the top of JA-Ile binding pocket of COI1, covering the JA-Ile trapped by COI1, and interacting with both COI1 and JA-Ile. Detailed analyses revealed that each amino acid in the LPIARR sequence interacts with JA-Ile by hydrogen-bond formation (LPIARR) or hydrophobic interaction (LPIARR). Thus, the change in any amino acid in conserved LPIAR(R/K) sequence will affect the affinity between JAZ and COI1-JA-Ile. Comparison of the amino acid sequences of the JAZ degron among the *Arabidopsis* functional JAZs showed small differences from LPIARR of JAZ1, which will be responsible for the difference in affinity for COI1-JA-Ile among the JAZs (K_d 7-34 for JA-Ile on fluorescence anisotropy assay).[34] Small differences in the *Arabidopsis* JAZ degron sequences are considered responsible for difference in their affinity.

In contrast, the degron sequence differences among functional *Sl*JAZs are smaller than those of *Arabidopsis* JAZs, but, nevertheless, each *Sl*JAZ binds with different affinities to *Sl*COI1-JA-Ile (**Figures 2 and 3 &Table 1**). Based on the results of the AlphaScreen assay, their affinities with *Sl*COI1-JA-Ile can be categorized into three groups: *Sl*JAZ1/5-8 of strong affinity (20> K_d), *Sl*JAZ2/3 of weak affinity (150> K_d), *Sl*JAZ4/9-11/13 of no/little affinity (K_d> 400). Especially, a large gap in affinity with *Sl*COI1-JA-Ile was observed among *Sl*JAZ1-4/13 in spite of no difference in their JAZ degron sequences.

We prepared the swapped *Sl*JAZPs and found that their affinity with SlCOI1-JA-Ile strongly depends on the extended JAZ degron sequence of VPQARKASLA or LPIARRXSLX (**Figures 4 and 5**).

The short degron sequence (V/L)P(Q/I)AR(R/K) has been hypothesized to play a critical role in hormone reception due to its high degree of conservation across numerous plant species. The only reported exception is the case of wild strawberry *Fragaris X ananassa* which uses the non-canonical JAZ degron sequence IPMQRK instead. Our result confirmed that tomato *Sl*JAZs employ the extended JAZ degron sequence of (V/L)P(Q/I)AR(R/K)XSLX for the perception of JA-Ile. The contribution of extended JAZ-degron sequence in the complex formation of *Sl*COI1-JAIle-*Sl*JAZs were further underpinned by using the *in silico* interaction models generated from reported crystal structure of *Arabidopsis* COI1-JAIle-JAZ1 (**Figure 6**). The DOD sequence in *Sl*JAZ formed strong hydron bond network with *Sl*COI1 to improve the stability of complex (**Figure 7**). In the interaction models of *Sl*COI1-JAIle-*Sl*JAZ1/5, the canonical JAZ degron of *Sl*JAZs retains the same interaction as that of *At*JAZs. Then, why do *Sl*JAZ1/2/3/4/13, which have LPIARR as a common canonical JAZ degron, have different affinities with *Sl*COI1-JA-Ile? Swapping experiments have shown that this is due to differences in the DOD sequence; when the DOD sequence of *Sl*JAZ1 was replaced with that of *Sl*JAZ3/4, the affinity was markedly decreased (*Sl*JAZ1-3/4DOD in **Figures 4a&5ab**). This indicates that the DOD sequence of *Sl*JAZ3/4 negatively affects the interaction with *Sl*COI1-JA-Ile. Specifically, two substitutions in the DOD sequence of *Sl*JAZ1, A166S and T168H/Y, are presumed to negatively affect the interaction between the LPIARR sequence and *Sl*COI1-JA-Ile. This is the first report to demonstrate that the longer sequences than canonical JAZ degron are employed for hormone perception of *Sl*COI1-*Sl*JAZ co-receptor.

*Sl*JAZ7 is unique among *Sl*JAZs having three amino acid residues in the extended JAZ degron (^{175}A, ^{176}M, and ^{181}T) which are not found in other *Sl*JAZs (**Figure 3a**). *Sl*JAZ7 has the extended JAZ degron sequence of LAMARRATLA in which the P(Q/I) in the canonical degaron (V/L)P(Q/I)AR(R/K) is replaced by ^{175}A^{176}M and the highly conserved S in the DOD sequence XSLX is replaced by ^{181}T. In the *Arabidopsis* COI1-JA-Ile-JAZ1 crystal structure, PI sequence in the canonical JAZ degaron of JAZ1 plays an important role in the interaction with COI1,[18] however, *Sl*JAZ7 lacking this sequence has a moderate affinity with K_d = 16.2 nM (**Table 1**). This suggests that *Sl*JAZ7 may interact with *Sl*COI1-JA-Ile in a manner different from other *Sl*JAZs.

Conclusion

A comprehensive study on ligand perception of *Sl*JAZ-*Sl*COI1 was performed. The results showed that the affinity of *Sl*JAZ for *Sl*COI-JA-Ile depends on the extended degron sequence, not on the canonical degron sequence. It was reported that *Sl*JAZ9-11of no affinity for *Sl*COI-JA-Ile is also JA-inducible,[23] suggesting that they have unique functions, such as suppression of JA signaling, in plant cells. Our new finding will provide further insight for the mechanism of hormone perception in edible tomato which leads to the genetic modification of of *Sl*COI1-*Sl*JAZ co-receptor to improve hormone perception and development of the synthetic agonist/antagonist.

Materials and Methods

All chemical reagents and solvents were obtained from commercial suppliers (Wako Pure Chemical Industries Co. Ltd., Nacalai Tesque Co., Ltd., Watanabe Chemical Industries Co. Ltd., Thermo Fisher Scientific K.K., GE Healthcare) and used without further purification. Coronatine (COR) and (+)-7-iso-JA-L-Ile (JA-Ile) were prepared according to the previous references.[1,35,36] DNA purification was performed using GENE PERP STAR PI-80X (KURABO, Osaka, Japan). Ultraviolet (UV)-visible spectra were recorded on a UV-2600 spectrophotometer (Shimadzu, Kyoto, Japan). The AlphaScreen assay was carried out on an EnVision (PerkinElmer, Inc., CA, US). SDS-PAGE and Western blotting were performed using a Mini-Protean III electrophoresis apparatus (Bio-Rad Laboratories, Inc., US), Tras-Blot Turbo (Bio-Rad Laboratories, Inc., US) and iBind Flex (Thermo Fisher Scientific K.K., CA, US). Chemiluminescent images were detected using the Amersham Imager 680 (GE Healthcare, CA, US). Reversed-phase high-performance liquid chromatography (HPLC) was performed on a PU-4180 plus with UV-4075 and MD-4010 detectors (JASCO, Tokyo, Japan). Absorbance at 220 nm and 488 nm was monitored by an MD-4010 photodiode array detector (PDA). MALDI-TOF MS analysis was performed on an Autoflex Max (Bruker Daltonics Inc., MA, US). The 3D structures were constructed using MOE 2020.09 software (Chemical Computing Groups, Montreal, Canada).

Preparation of the *Sl*COI1 and *Sl*JAZs proteins

Standard methods for cloning were used, and PCR-amplified DNA fragments were sequenced after cloning into the vectors. The plasmids of GST-fused AtCOI1 or AtASK1 (pFB-GTE-COI1 and pFB-HTB-ASK1) were obtained from Addgene (https://www.addgene.org/), and the plasmid for wheat-derived cell-free protein expression system (pEU-FLAG-GW-STOP) was kindly gifted from Drs. Koji Miyamoto (Teikyo University), Kazunori Okada (The University of Tokyo), and Tatsuya Sawasaki (Ehime University). The full-length CDS of *Sl*COI1 was obtained from Osaka Prefecture University (kindly supported by Prof. Koh Aoki) and was cloned into pFB-GTE-COI1 to prepare the plasmid of GST-fused *Sl*COI1. These *Sl*COI1 and *At*ASK1 proteins were co-expressed in insect cells and purified by Glutathione Sepharose 4B (GE Healthcare) according to the previous reports.[18,34,37] The full-length CDS of *Sl*JAZ2/3/5/6/7 were obtained from Osaka Prefecture University (kindly supported by Prof. Koh Aoki), and was PCR-amplified and cloned into the pDONR221 vector (Invitrogen, CA, US) by using BP reaction (Gateway®). Coding sequences of *Sl*JAZ1/4 were isolated from *Solanum* cDNA using the primers. PCR-amplified *Sl*JAZ1/4 DNA was cloned into pENTR/D-TOPO (Thermo Fisher Scientific, USA). Coding sequences of *Sl*JAZ8/9/10/11/13 were synthesized by the manufacturers (Eurofins Genomics K.K., Japan), and were cloned into the pDONR221 vector using the BP reaction. The CDS was then inserted into pEU-FLAG-GW-STOP vector by using the LR reaction (Gateway®) to prepare the plasmid for FLAG tag-fused *Sl*JAZ (pEU-FLAG-GW-*Sl*JAZs). These *Sl*JAZs proteins were expressed in wheat germ-derived cell-free protein expression system according to the previous reports,[38] and used without purification. Cell-free translation reaction was performed according to the instruction protocol (Cell Free Sciences, Co., Ltd., Ehime, Japan) with minor modification. Briefly, the transcription reactions with pEU-FLAG-GW-*Sl*JAZs (each 1 μg) were performed at 37 ºC for 5 h. The obtained mixture of mRNA was added to creatine kinase and WEPRO7240 solution to prepare the translation mixture, and it was carefully transferred to the bottom of a well containing translation buffer to form the bilayer reaction, and then incubated at 15 ºC for 20 h in 96 wells plate. The obtained protein mixture was centrifuged (20,000 g for 15 min at 4 ºC) and the supernatant was used for the pulldown experiments without any purification.

Synthesis of Fl-*Sl*JAZPs

All *Sl*JAZ peptides were prepared by microwave-assisted solid phase synthesis with Fmoc-Tyr-Wang resin (90 μm) using Initiator+ Alstra (Biotage Ltd, North Carolina, US) as previously reported with minor modification.[34] A representative protocol is as follows. The resin was swollen in DMF at 70ºC for 20 min. The Fmoc protecting group was removed by treating with 20% piperidine in DMF twice. Amino acid coupling was accomplished by mixing the resin with Fmoc protected amino acids (3 eq), *O*-(*1H*-Benzotriazol-1-yl)-*N,N,N′,N′*-tetramethyluronium hexafluorophosphate (HBTU, 3 eq), 1-Hydroxy-*1H*-benzotriazole hydrate (HOBt•H_2O) (3 eq), and DIPEA (6 eq) in DMF, and subjecting it to microwave irradiation at 50ºC for either 30 min (Fmoc-Arg-OH) or 10 min (others except for Fmoc-Arg-OH). After the peptide had been fully elongated, solid phase-peptide was mixed with 5-carboxy- fluorescein diacetate (3 eq), HBTU (5 eq) and DIPEA (5 eq) in DMF and incubated at r.t. for 2 h. After the reaction, the peptide was deprotected by stirring using TFA solution at r.t. for 1.5 h (in cases of SlJAZ6 or 7, deprotection was performed with TFA solution containing thioanisole, anisole and 1,2-ethanedithiol for the avoidance of methionine oxidation). The reaction mixture was purified by HPLC using a Develosil ODS-HG-5 column (Φ 4.6×250 mm) eluting with a linear gradient (CH_3CN (0.05% TFA):H_2O (0.05% TFA) = 20:80 (5 min) to 50:50 (35 min)) to afford fluorescein-conjugated *Sl*JAZ peptide. After lyophilization, conjugated *Sl*JAZ peptide was dissolved in sterilized water to prepare the stock solution. The concentrations of the stock solution were determined by their absorbance at 494 nm in 0.1 N NaOH aqueous solution using a molar extinction coefficient of 75,000 M^{-1} cm^{-1}. The purity of each peptide was confirmed by HPLC analyses, and these were characterized by MALDI-TOF MS as follows;

Fl-SlJAZ1: m/z $[M+H]^+$ calcd for 3571,92, found 3571.92

Fl-SlJAZ2: m/z $[M+H]^+$ calcd for 3573.86, found 3573.86

Fl-SlJAZ3: m/z $[M+H]^+$ calcd for 3623.92, found 3623.90

Fl-SlJAZ4: m/z $[M+H]^+$ calcd for 3651.85, found 3651.85

Fl-SlJAZ5: m/z $[M+H]^+$ calcd for 3429.81, found 3429.80

Fl-SlJAZ6: m/z $[M+H]^+$ calcd for 3500.83, found 3500.83

Fl-SlJAZ7: m/z $[M+H]^+$ calcd for 3594.97, found 3594.99

Fl-SlJAZ8: m/z $[M+H]^+$ calcd for 3443.80, found 3443.76

Fl-SlJAZ9: m/z $[M+H]^+$ calcd for 3515.88, found 3515.84

Fl-SlJAZ10: m/z $[M+H]^+$ calcd for 3656.97, found 3656.99

Fl-SlJAZ11: m/z $[M+H]^+$ calcd for 3605.90, found 3605.89

Fl-SlJAZ13: m/z $[M+H]^+$ calcd for 3729.97, found 3729.98

Fl-SlJAZ1/2/4-5: m/z $[M+H]^+$ calcd for 3500.87, found 3500.84

Fl-SlJAZ1-3DOD: m/z $[M+H]^+$ calcd for 3623.92, found 3623.93

Fl-SlJAZ1-4DOD: m/z $[M+H]^+$ calcd for 3649.93, found 3649.92

Fl-SlJAZ2-5DOD: m/z $[M+H]^+$ calcd for 3500.84, found 3500.84

Fl-SlJAZ5-2DOD: m/z $[M+H]^+$ calcd for 3502.82, found 3502.82

Fl-SlJAZ2-5: m/z $[M+H]^+$ calcd for 3429.81, found 3429.80

Fl-SlJAZ5-2: m/z $[M+H]^+$ calcd for 3573.86, found 3573.87

Pulldown assay

All chemicals (JA-Ile or COR) were dissolved in ethanol to generate 10 mM stock solutions and diluted with 20% ethanol aq. for preparation of 100 μM stock solutions. For the pull-down experiments using full-length *Sl*JAZ proteins, purified GST-COI1 (5 nM), FLAG-tagged *Sl*JAZ (each 20 μL of the translation mixture), and the ligands (COR or JA-Ile) in 350 μL of incubation buffer (50 mM Tris-HCl buffer, pH 7.8, 100 mM NaCl, 20 mM 2-mercaptoethanol, 10% glycerol, 0.1% Tween20, 100 nM inositol-1,2,4,5,6-pentakisphosphate (IP5)) were combined with anti-FLAG antibody (0.2 μL, Sigma Aldrich, F1804, clone M2), and incubated for 10–15 h at 4ºC with rotation. After incubation, the samples were combined with SureBeads™ Protein G (10 μL in 50% incubation buffer slurry, Bio-Rad). After 3 h incubation at 4ºC with rotation, the samples were washed three times with 350 μL of fresh incubation buffer. The washed beads were resuspended in 35 μL of SDS-PAGE loading buffer containing dithiothreitol (DTT, 100 mM). After heating for 10 min at 60 ºC, the samples were subjected to SDS-PAGE and analyzed by western blotting. The bound GST-COI1 protein was detected using anti-GST HRP conjugate (RPN1236, GE Healthcare, 5,000-fold dilution in blocking buffer (Nakalai tesque, Inc., Japan)). FLAG-JAZ proteins were detected using anti-FLAG antibody (1,000-fold dilution in blocking buffer) and anti-mouse IgG-HRP antibody (Southern Biotech. Inc., Birmingham, US, 1031-05, 20,000-fold dilution in blocking buffer). Three independent replicates were done with similar results.

For the pull-down experiments using fluorescein-tagged *Sl*JAZ peptides (Fl-

*Sl*JAZps), purified GST-COI1 (5 nM), Fl-*Sl*JAZp (10 nM), and JA-Ile (1 μM) in 350 μL of incubation buffer were combined with anti-fluorescein antibody (0.2 μL, GeneTex, CA, US), and incubated for 10–15 h at 4ºC with rotation. After incubation, the samples were combined with SureBeads^{TM} Protein G (10 μL in 50% incubation buffer slurry, Bio-Rad). The washing and eluting protocols were same as the pulldown experiments using full-length JAZ proteins. Three independent replicates were done with similar results.

AlphaScreen Assay

AlphaScreen experiments were performed at 25 °C in the incubation buffer. 15 μL of the reaction mixture containing the incubation buffer, 5 nM *Sl*COI1, 10 nM Fl-*Sl*JAZPs and various concentrations of COR or JA-Ile was added to a 1/2 Area AlphaPlate^{TM}-96 (PerkinElmer), and then incubated for 1 h at 4ºC. Then, 10 μL of a detection mixture containing incubation buffer, 0.1 μL of FITC-coated donor beads, 0.1 μL of GST-coated acceptor beads was added to each well. Finally, the mixture was incubated for 12 h and the luminescence signals were detected using the Envision 2105 Multimode Plate Reader (PerkinElmer). The experiment was repeated three times, and the data are presented as average values with standard deviation.

***In silico* analyses**

The homology modeling of SlCOI1 was obtained based on the crystal structure of *At*COI1–JA-Ile–*At*JAZ1 (PDB ID: 3OGL). The structure preparation program in MOE 2020.09 was used to deduce the structures of the absent residues (residues 550–562) of *At*COI1. The model structures of *Sl*JAZ1, and 5 were constructed by mutating residues of the *At*JAZ1 peptide of the complex.

The MD simulations of the *Sl*COI1-JA-Ile-*Sl*JAZ1 and the *Sl*COI1-JA-Ile-*Sl*JAZ5 were performed under the constant temperature and pressure (T = 300 K, P = 1 atm) condition. The Parrinello-Rahman type thermostat [Parrinello, M. & Rahman, A. Polymorphic transitions in single crystals: A new molecular dynamics method. Journal of Applied Physics 52, 7182-7190 (1981).] and the Nosé-Hoover barostat [Hoover, W.G. Canonical dynamics: Equilibrium phase-space distributions. Physical Review A 31, 1695-1697 (1985).] were adopted to control the system temperature and pressure, respectively. The Amber14SB [James A. Maier, Carmenza Martinez, Koushik Kasavajhala, Lauren

Wickstrom, Kevin E. Hauser, and Carlos Simmerling, "ff14SB: Improving the Accuracy of Protein Side Chain and Backbone Parameters from ff99SB", J. Chem. Theory Comput. 2015, 11, 8, 3696–3713] and the generalized amber force field (gaff) [Junmei, W., M., W.R., W., C.J., A., K.P. & A., C.D. Development and testing of a general amber force field. Journal of Computational Chemistry 25, 1157-1174 (2004)] were assigned for the protein/peptide and the ligand molecule, respectively. The TIP3P model [Jorgensen, W.L., Chandrasekhar, J., Madura, J.D., Impey, R.W. & Klein, M.L. Comparison of simple potential functions for simulating liquid water. The Journal of Chemical Physics 79, 926-935 (1983).] was used for water solvent. The cutoff length for van der Waals (vdW) and coulomb interactions in real space was 12 Å. The particle mesh Ewald (PME) method [Darden, T., York, D. & Pedersen, L. Particle mesh Ewald: An N·log(N) method for Ewald sums in large systems. The Journal of Chemical Physics 98, 10089-10092 (1993).] was used for the estimation of the coulomb interactions. The time step for integration of equations of motions was 2 fs. All MD calculations were done by GROMACS2018 program [M.J. Abraham, T. Murtola, R. Schulz, S. Pall, J.C. Smith, B. Hess, E. Lindahl, GROMACS: High performance molecular simulations through multi-level parallelism from laptops to supercomputers, SoftwareX 1, 19-25 (2015)].

The snapshot structures of the *Sl*COI1-JA-Ile-*Sl*JAZ1 and *Sl*COI1-JA-Ile-*Sl*JAZ5 were sampled every 10 ps. We first performed 10 ns MD simulations for energy minimization/equilibration of the systems and then conducted five independent 100 ns MD simulations (total 500 ns) for each system. The system equilibrations of the protein/peptide and the ligand were monitored by the root means square displacement (RMSD) values as the simulation time step. We confirmed that the ligand binding modes were not largely changed in all MD simulations. The last snapshot structures were used as the representative structures to investigate the binding forms of the complex.

Acknowledgement

This work was financially supported by a Grant-in-Aid for Scientific Research from JSPS, Japan (nos. 17H06407, 18KK0162, and 20H00402 for MU, nos. 18H02101 and 19H05283 for YT, and nos. 19K05378 and 20H04791 for HS), JSPS A3 Foresight Program (MU), and JSPS Core-to-Core Program Asian Chemical Biology Initiative (MU).

And we also thank to Mr. Teppei Kamimura for his technical help. The computations in this study were performed using the Advanced Center for Computing and Communication of RIKEN, Research Center for Computational Science of Institute for Molecular Science (IMS), Research Center for Advanced Computing Infrastructure of Japan Advanced Institute of Science and Technology (JAIST).

Author contribution

M.U. conceived, designed, and coordinated the research project. M.U., Y.T., R.S., K.H., and H.S. designed the experiments and examined data. R.S., K.H., M.N., H.N., S.Y., and T.M. performed the wet experiments. H.S., Y.T., and K.H. performed *in silico* studies. M.U., Y.T., K.H., and R.S. wrote the main manuscript text and all figures. All authors reviewed the manuscript.

Conflicts of interest

There are no conflicts to declare.

1 Fonseca, S. *et al.* (+)-7-iso-Jasmonoyl-L-isoleucine is the endogenous bioactive jasmonate. *Nature Chemical Biology* **5**, 344-350, doi:10.1038/nchembio.161 (2009).

2 Wasternack, C. & Song, S. Jasmonates: biosynthesis, metabolism, and signaling by proteins activating and repressing transcription. *Journal of Experimental Botany* **68**, 1303-1321, doi:10.1093/jxb/erw443 (2017).

3 Wasternack, C. Jasmonates: an update on biosynthesis, signal transduction and action in plant stress response, growth and development. *Annals of Botany* **100**, 681-697, doi:10.1093/aob/mcm079 (2007).

4 Wasternack, C. & Hause, B. Jasmonates: biosynthesis, perception, signal transduction and action in plant stress response, growth and development. An update to the 2007 review in Annals of Botany. *Annals of Botany* **111**, 1021-1058, doi:10.1093/aob/mct067 (2013).

5 Pauwels, L. & Goossens, A. The JAZ proteins: a crucial interface in the jasmonate signaling cascade. *Plant Cell* **23**, 3089-3100, doi:10.1105/tpc.111.089300 (2011).

6 Kazan, K. & Manners, J. M. JAZ repressors and the orchestration of phytohormone crosstalk. *Trends in Plant Science* **17**, 22-31, doi:10.1016/j.tplants.2011.10.006 (2012).

7 Zhang, F. *et al.* Structural basis of JAZ repression of MYC transcription factors in jasmonate signalling. *Nature* **525**, 269-273, doi:10.1038/nature14661 (2015).

8 Pauwels, L. *et al.* NINJA connects the co-repressor TOPLESS to jasmonate signalling. *Nature* **464**, 788-791, doi:10.1038/nature08854 (2010).

9 Bai, Y., Meng, Y., Huang, D., Qi, Y. & Chen, M. Origin and evolutionary analysis of the plant-specific TIFY transcription factor family. *Genomics* **98**, 128-136, doi:10.1016/j.ygeno.2011.05.002 (2011).

10 Chini, A. *et al.* The JAZ family of repressors is the missing link in jasmonate signalling. *Nature* **448**, 666-671, doi:10.1038/nature06006 (2007).

11 Thines, B. *et al.* JAZ repressor proteins are targets of the SCF(COI1) complex during jasmonate signalling. *Nature* **448**, 661-665, doi:10.1038/nature05960 (2007).

12 Yan, Y. *et al.* A downstream mediator in the growth repression limb of the

jasmonate pathway. *Plant Cell* **19**, 2470-2483, doi:10.1105/tpc.107.050708 (2007).

13 Chini, A., Gimenez-Ibanez, S., Goossens, A. & Solano, R. Redundancy and specificity in jasmonate signalling. *Current Opinion in Plant Biology* **33**, 147-156, doi:http://dx.doi.org/10.1016/j.pbi.2016.07.005 (2016).

14 Gimenez-Ibanez, S. *et al.* JAZ2 controls stomata dynamics during bacterial invasion. *New Phytol* **213**, 1378-1392, doi:10.1111/nph.14354 (2017).

15 Major, I. T. *et al.* Regulation of growth-defense balance by the JASMONATE ZIM-DOMAIN (JAZ)-MYC transcriptional module. *New Phytol*, doi:10.1111/nph.14638 (2017).

16 Guo, Q. *et al.* JAZ repressors of metabolic defense promote growth and reproductive fitness in Arabidopsis. *Proc Natl Acad Sci U S A* **115**, E10768-E10777, doi:10.1073/pnas.1811828115 (2018).

17 Demianski, A. J., Chung, K. M. & Kunkel, B. N. Analysis of Arabidopsis JAZ gene expression during Pseudomonas syringae pathogenesis. *Molecular plant pathology* **13**, 46-57, doi:10.1111/j.1364-3703.2011.00727.x (2012).

18 Sheard, L. B. *et al.* Jasmonate perception by inositol-phosphate-potentiated COI1-JAZ co-receptor. *Nature* **468**, 400-405, doi:10.1038/nature09430 (2010).

19 Garrido-Bigotes, A., Valenzuela-Riffo, F. & Figueroa, C. R. Evolutionary Analysis of JAZ Proteins in Plants: An Approach in Search of the Ancestral Sequence. *International Journal of Molecular Sciences* **20**, 5060 (2019).

20 Garrido-Bigotes, A. *et al.* A new functional JAZ degron sequence in strawberry JAZ1 revealed by structural and interaction studies on the COI1-JA-Ile/COR-JAZs complexes. *Sci Rep* **10**, 11310, doi:10.1038/s41598-020-68213-w (2020).

21 Sen, S., Kundu, S. & Dutta, S. K. Proteomic analysis of JAZ interacting proteins under methyl jasmonate treatment in finger millet. *Plant Physiology and Biochemistry* **108**, 79-89, doi:https://doi.org/10.1016/j.plaphy.2016.05.033 (2016).

22 Takaoka, Y. *et al.* A comprehensive in vitro fluorescence anisotropy assay system for screening ligands of the jasmonate COI1-JAZ co-receptor in plants. *J Biol Chem* **294**, 5074-5081, doi:10.1074/jbc.RA118.006639 (2019).

553 23 Chini, A., Ben-Romdhane, W., Hassairi, A. & Aboul-Soud, M. A. M.
554 Identification of TIFY/JAZ family genes in Solanum lycopersicum and their
555 regulation in response to abiotic stresses. *PloS one* **12**, e0177381,
556 doi:10.1371/journal.pone.0177381 (2017).
557 24 Ishiga, Y., Ishiga, T., Uppalapati, S. R. & Mysore, K. S. Jasmonate ZIM-domain
558 (JAZ) protein regulates host and nonhost pathogen-induced cell death in tomato
559 and Nicotiana benthamiana. *PloS one* **8**, e75728,
560 doi:10.1371/journal.pone.0075728 (2013).
561 25 Sun, J. Q., Jiang, H. L. & Li, C. Y. Systemin/Jasmonate-mediated systemic
562 defense signaling in tomato. *Mol Plant* **4**, 607-615, doi:10.1093/mp/ssr008 (2011).
563 26 Li, H. *et al.* Efficient ASK-assisted system for expression and purification of plant
564 F-box proteins. *Plant J* **92**, 736-743, doi:10.1111/tpj.13708 (2017).
565 27 Melcher, K. *et al.* A gate-latch-lock mechanism for hormone signalling by abscisic
566 acid receptors. *Nature* **462**, 602-608, doi:10.1038/nature08613 (2009).
567 28 Nakamura, Y. *et al.* Synthesis of 6-substituted 1-oxoindanoyl isoleucine
568 conjugates and modeling studies with the COI1-JAZ co-receptor complex of lima
569 bean. *Journal of Chemical Ecology* **40**, 687-699, doi:10.1007/s10886-014-0469-
570 2 (2014).
571 29 Valenzuela-Riffo, F., Garrido-Bigotes, A., Figueroa, P. M., Morales-Quintana, L.
572 & Figueroa, C. R. Structural analysis of the woodland strawberry COI1-JAZ1 co-
573 receptor for the plant hormone jasmonoyl-isoleucine. *Journal of molecular*
574 *graphics & modelling* **85**, 250-261, doi:10.1016/j.jmgm.2018.09.004 (2018).
575 30 Tian, J. *et al.* The OsJAZ1 degron modulates jasmonate signaling sensitivity
576 during rice development. *Development* **146**, dev173419, doi:10.1242/dev.173419
577 (2019).
578 31 Shyu, C. *et al.* JAZ8 lacks a canonical degron and has an EAR motif that mediates
579 transcriptional repression of jasmonate responses in Arabidopsis. *Plant Cell* **24**,
580 536-550, doi:10.1105/tpc.111.093005 (2012).
581 32 Thireault, C. *et al.* Repression of jasmonate signaling by a non-TIFY JAZ protein
582 in Arabidopsis. *Plant Journal* **82**, 669-679, doi:10.1111/tpj.12841 (2015).
583 33 Moreno, J. E. *et al.* Negative feedback control of jasmonate signaling by an

alternative splice variant of JAZ10. *Plant Physiology* **162**, 1006-1017, doi:10.1104/pp.113.218164 (2013).

34 Takaoka, Y., Hayashi, K., Suzuki, K., Azizah, I. N. & Ueda, M. in *Jasmonate in Plant Biology: Methods and Protocols* (eds Antony Champion & Laurent Laplaze) 145-160 (Springer US, 2020).

35 Kato, N. *et al.* A scalable synthesis of (+)-coronafacic acid. *Chirality* **32**, 423-430, doi:10.1002/chir.23172 (2020).

36 Okada, M. *et al.* Total syntheses of coronatines by exo-selective Diels-Alder reaction and their biological activities on stomatal opening. *Organic & biomolecular chemistry* **7**, 3065-3073, doi:10.1039/b905159g (2009).

37 Takaoka, Y. *et al.* A rationally designed JAZ subtype-selective agonist of jasmonate perception. *Nat Commun* **9**, 3654, doi:10.1038/s41467-018-06135-y (2018).

38 Sawasaki, T. *et al.* A bilayer cell-free protein synthesis system for high-throughput screening of gene products. *FEBS Letters* **514**, 102-105, doi:https://doi.org/10.1016/S0014-5793(02)02329-3 (2002).

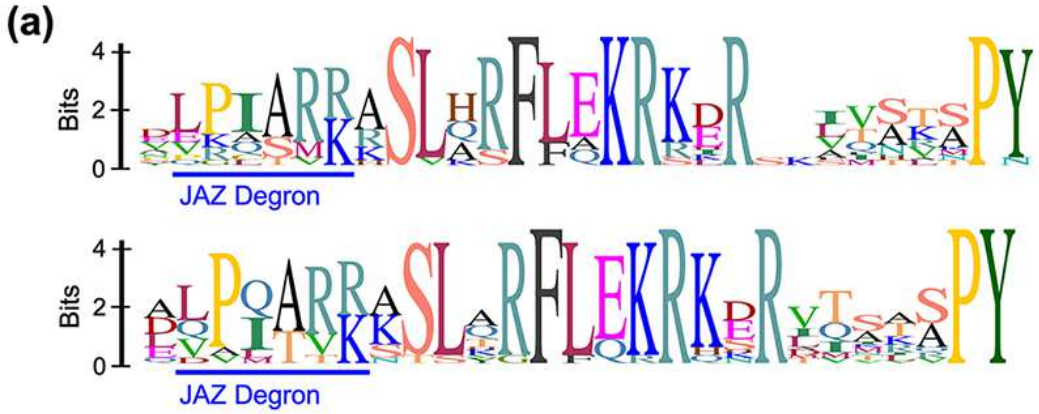

(b)

*At*JAZ1:	^{201}L	P	I	A	R	R
*At*JAZ2:	^{203}L	P	I	A	R	R
*At*JAZ3:	^{301}L	P	L	A	R	K
*At*JAZ4:	^{228}L	P	Q	T	R	K
*At*JAZ5:	^{180}E	R	I	A	R	R
*At*JAZ6:	^{184}E	R	I	A	R	R
*At*JAZ7:	^{119}Q	K	A	S	M	K
*At*JAZ8:	^{102}P	K	A	S	M	K
*At*JAZ9:	^{219}V	P	Q	A	R	K
*At*JAZ10:	^{167}L	P	I	A	R	R
*At*JAZ11:	^{196}V	P	I	A	R	R
*At*JAZ12:	^{138}L	P	I	A	R	R
*At*JAZ13:	^{83}L	G	C	S	V	K

*Sl*JAZ1:	^{160}L	P	I	A	R	R
*Sl*JAZ2:	^{197}L	P	I	A	R	R
*Sl*JAZ3:	^{250}L	P	I	A	R	R
*Sl*JAZ4:	^{154}L	P	I	A	R	R
*Sl*JAZ5:	^{328}V	P	Q	A	R	K
*Sl*JAZ6:	^{281}V	P	Q	A	R	K
*Sl*JAZ7:	^{174}L	A	M	A	R	R
*Sl*JAZ8:	^{193}V	P	Q	A	R	K
*Sl*JAZ9:	^{85}Q	P	Q	T	V	K
*Sl*JAZ10:	^{76}Q	P	Q	T	V	K
*Sl*JAZ11:	^{112}Q	P	Q	T	V	K
*Sl*JAZ12:	^{86}D	V	L	T	T	R
*Sl*JAZ13:	^{338}L	P	I	A	R	R

Figure 1. (a) Sequence logos of the Jas motif of *At*JAZs (top) or *Sl*JAZs (bottom). **(b)** The canonical JAZ degron sequences of *At*JAZs (left) and *Sl*JAZs (right).

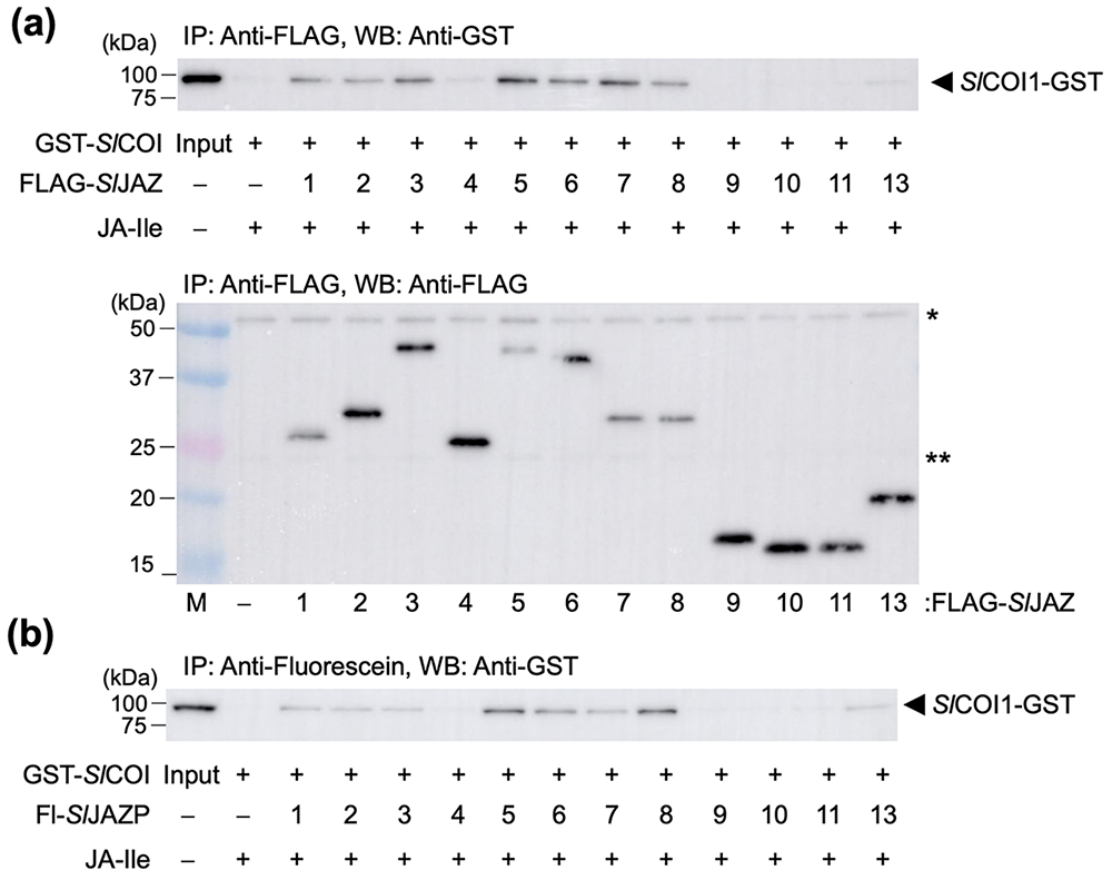

606

607

608 **Figure 2.** (a) Pull down assay of GST-*Sl*COI1 with FLAG-*Sl*JAZ (full-length proteins)
609 in the presence of JA-Ile (100 nM). GST-*Sl*COI1 bound to FLAG-*Sl*JAZ proteins was
610 pulled down with anti-FLAG antibody and Protein G magnetic beads, and analyzed by
611 immunoblotting (top: anti-GST-HRP conjugate for detection of GST-*Sl*COI1, bottom:
612 anti-FLAG antibody and anti mouse-IgG HRP conjugate for detection of FLAG-*Sl*JAZs).
613 * or ** show the bands derived from heavy chain or light chain of the anti-FLAG antibody.
614 (b) Pull down assay of GST-*Sl*COI1 with Fl-*Sl*JAZPs in the presence of JA-Ile (100 nM).
615 GST-*Sl*COI1 bound to Fl-*Sl*JAZPs was pulled down with anti-fluorescein antibody and
616 Protein G magnetic beads, and analyzed by immunoblotting (anti-GST-HRP conjugate
617 for detection of GST-*Sl*COI1).

618

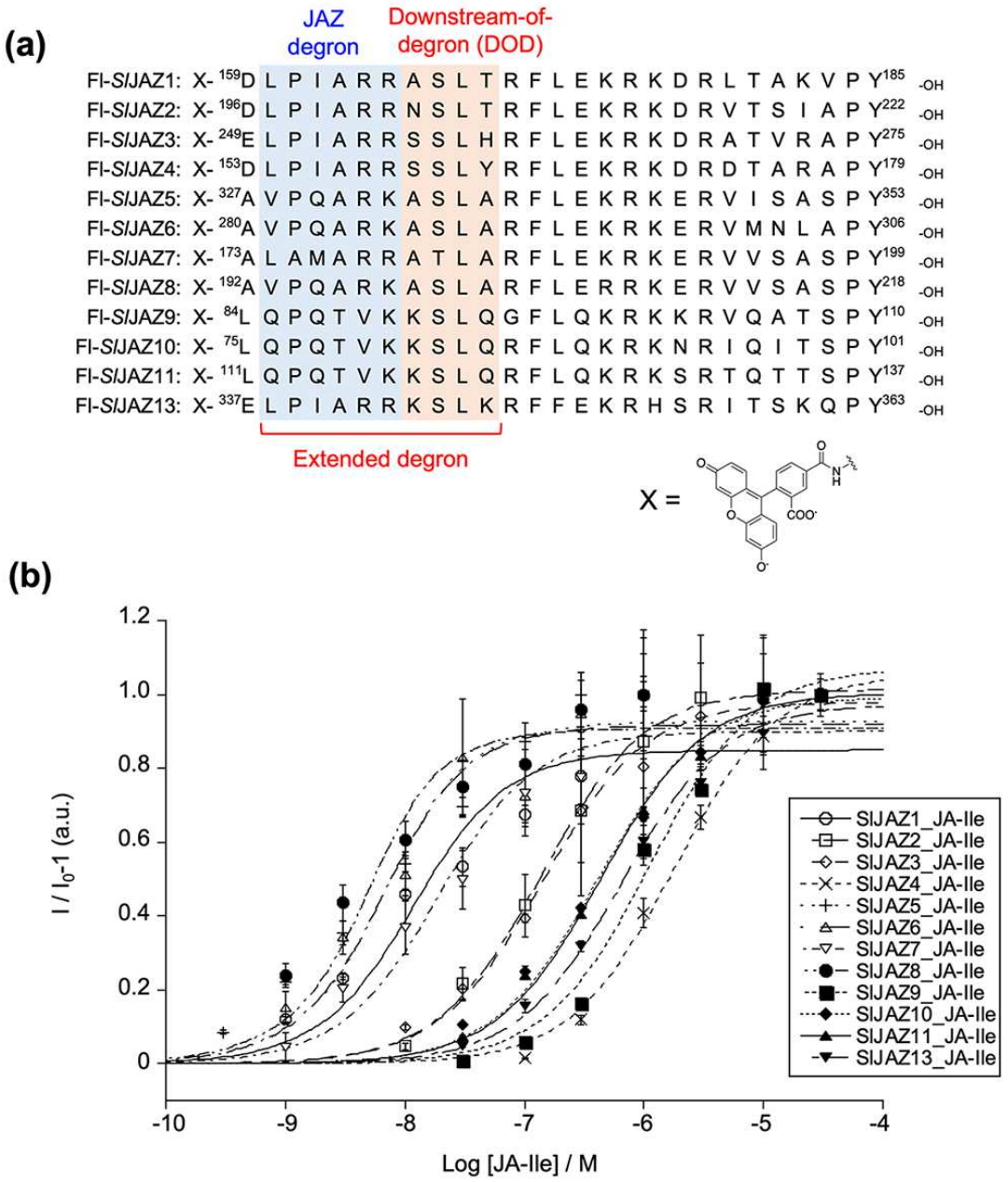

Figure 3. (a) Chemical structures of fluorescein-tagged *Sl*JAZ1-11/13 degron short peptides (*Sl*JAZP1-11/13). The canonical JAZ degron sequences were shown in blue frame and down-stream-of-degron (DOD) sequence were in orange frame. (b) AlphaScreen assays using Fl-*Sl*JAZPs and GST-*Sl*COI1 with JA-Ile (0 – 30 μM). Experiments were performed in triplicate to obtain mean and S.D. (shown as error bars).

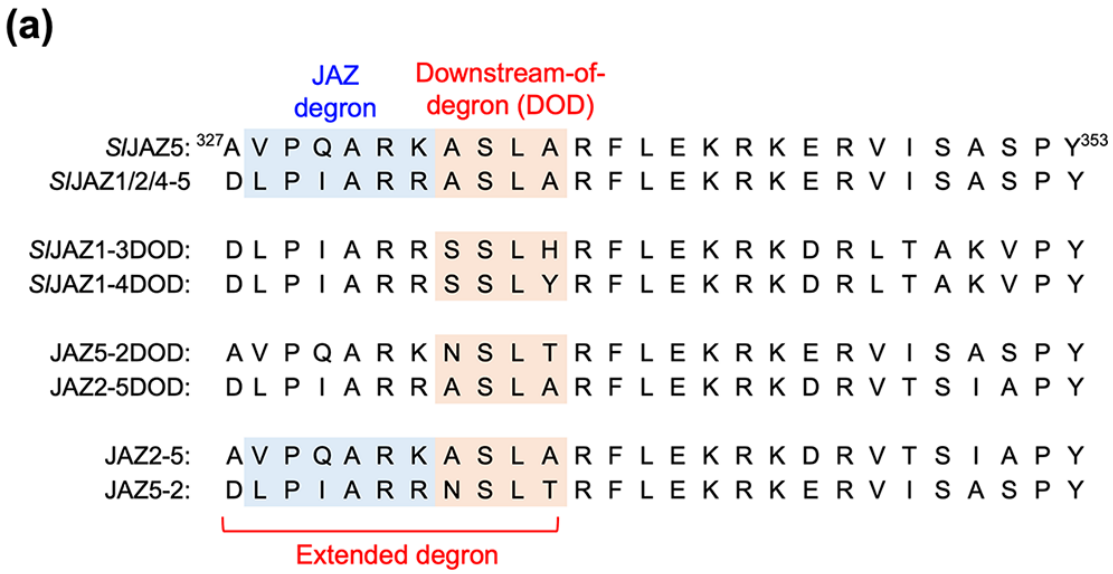

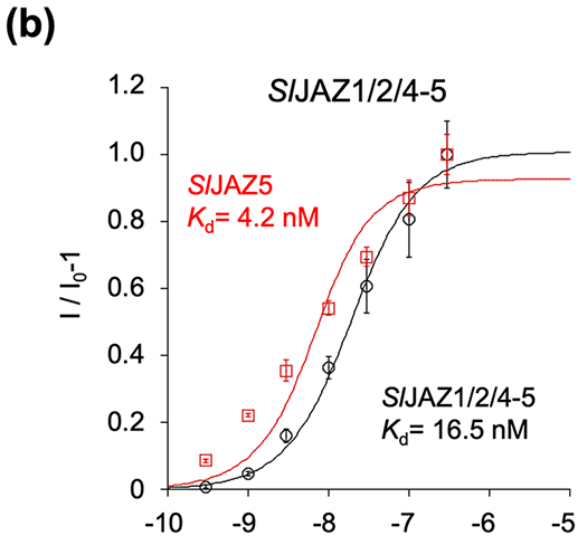

627
628

629 **Figure 4.** (a) Design of the swapped *Sl*JAZ peptides (*Sl*JAZ5, 1/2/4-5, 1-3DOD, 1-4DOD
630 5-2DOD, 2-5DOD, 2-5, 5-2). The canonical JAZ degron sequences were shown in blue
631 frame and down-stream-of-degron (DOD) sequence were in orange frame. (b)
632 AlphaScreen assay using GST-*Sl*COI1 and Fl-*Sl*JAZP1/2/4-5 (black circle) or Fl-*Sl*JAZ5
633 (red square) with JA-Ile (0 – 300 nM). Experiments were performed in triplicate to obtain
634 mean and S.D. (shown as error bars).

635

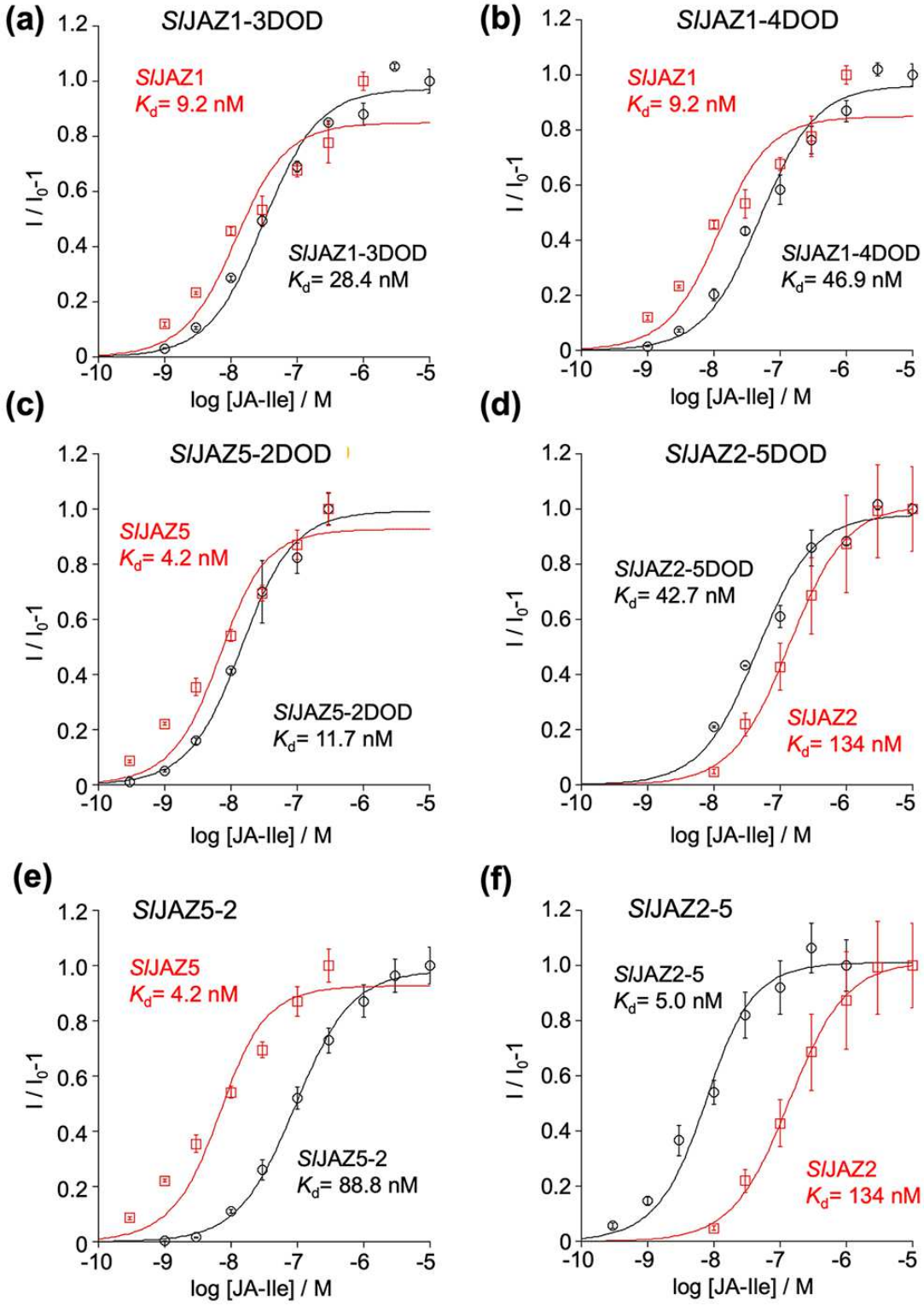

Figure 5. Alphascreen assay of swapped Fl-*Sl*JAZPs (a: SlJAZ1-3DOD, b: 1-4DOD, c: 5-2DOD, d: 2-5DOD, e: 5-2, f: 2-5) to consider the extended degron sequence. Signal

640 intensity change of AlphaScreen of swapped Fl-*Sl*JAZPs and GST-*Sl*COI1 upon addition
641 of JA-Ile (0-10 μM). Black circles show the results of swapped *Sl*JAZPs and red squares
642 show those of corresponding natural *Sl*JAZPs, respectively. Experiments were performed
643 in triplicate to obtain mean and S.D. (shown as error bars).
644

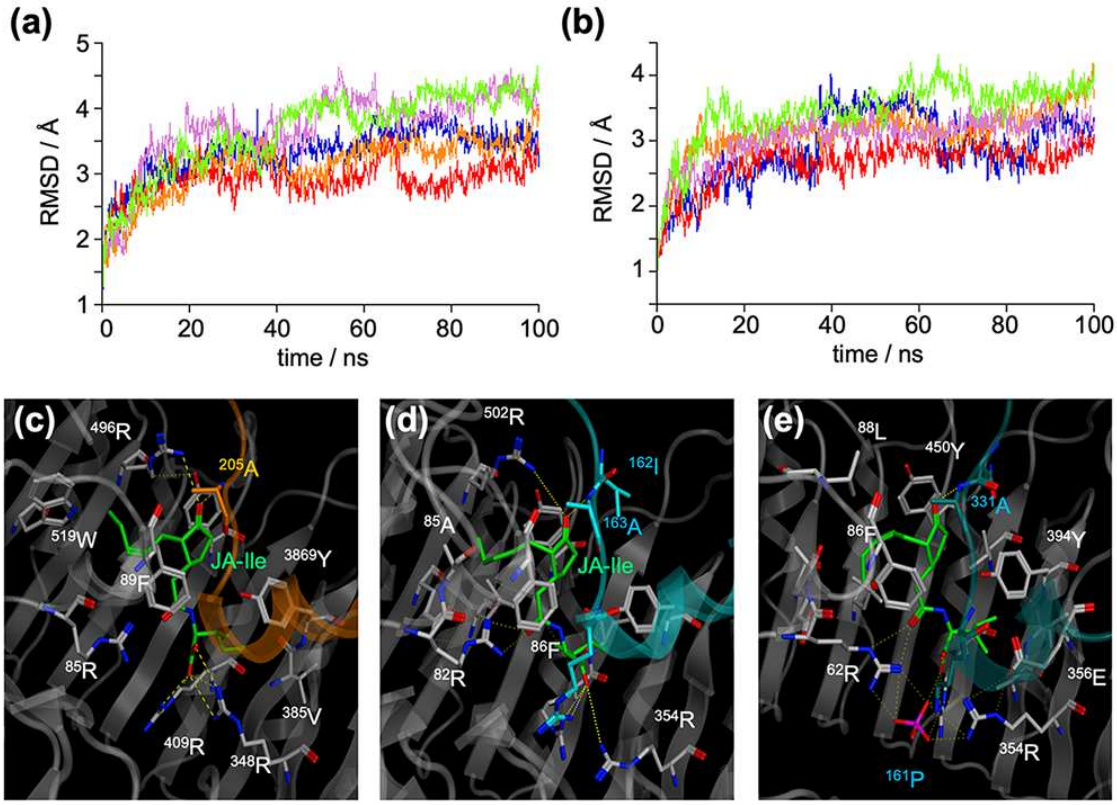

Figure 6. (a, b) The RMSDs of backbone atoms of the complex of *Sl*COI1-JA-Ile-*Sl*JAZ1 (a) and *Sl*COI1-JA-Ile-*Sl*JAZ5 (b) as a function of MD time step. (c) The reported structure of the ligand binding pocket of *At*COI1-JA-Ile-*At*JAZ1 (PDB ID: 3OGL). (d, e) The representative structure of the ligand binding pocket of *Sl*COI1-JA-Ile-*Sl*JAZ1 (d) and that of *Sl*COI1-JA-Ile-*Sl*JAZ5 (e), which was obtained by homology modeling and MD simulation.

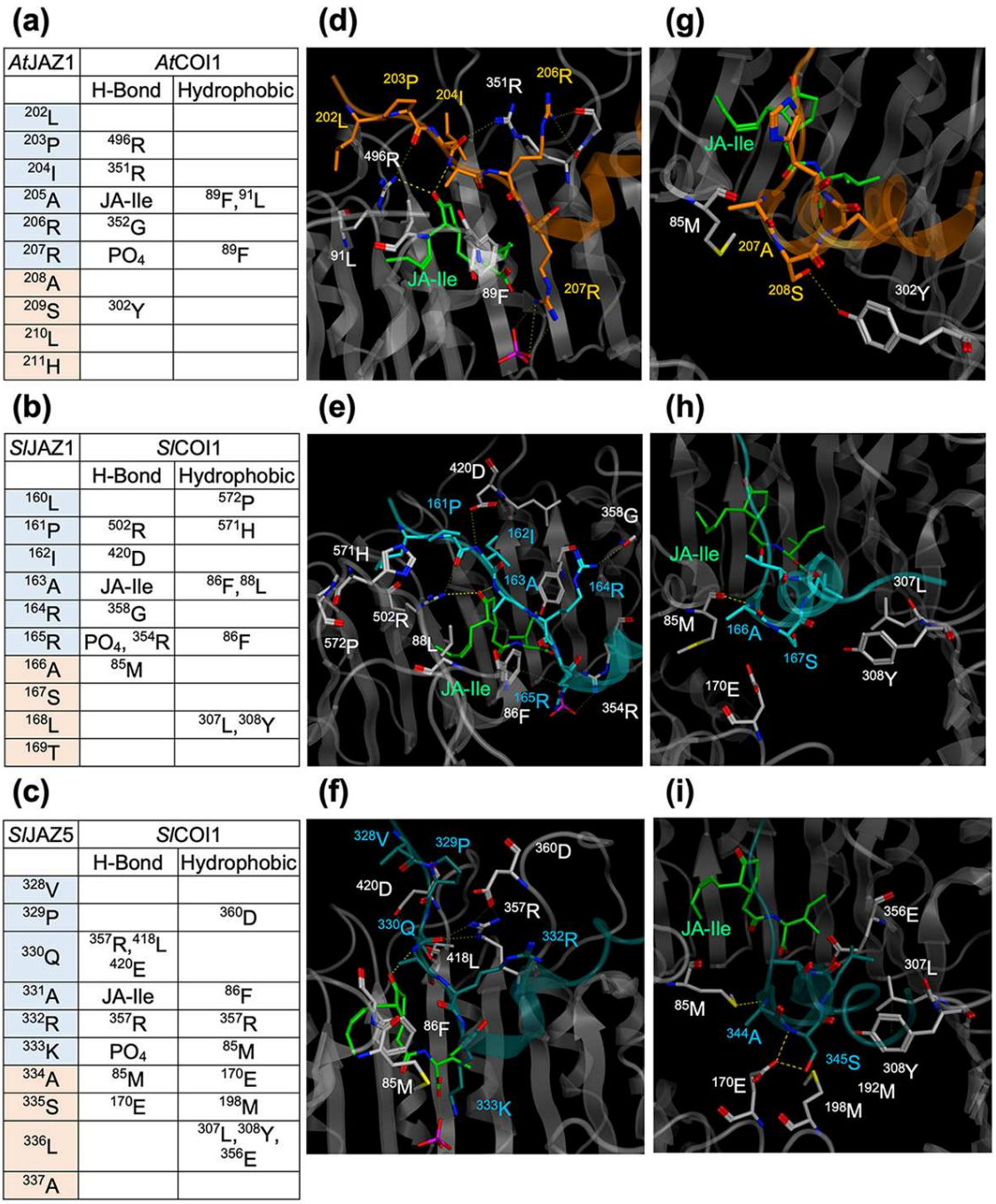

*At*JAZ1	*At*COI1	
	H-Bond	Hydrophobic
^{202}L		
^{203}P	^{496}R	
^{204}I	^{351}R	
^{205}A	JA-Ile	^{89}F, ^{91}L
^{206}R	^{352}G	
^{207}R	PO_4	^{89}F
^{208}A		
^{209}S	^{302}Y	
^{210}L		
^{211}H		

*Sl*JAZ1	*Sl*COI1	
	H-Bond	Hydrophobic
^{160}L		^{572}P
^{161}P	^{502}R	^{571}H
^{162}I	^{420}D	
^{163}A	JA-Ile	^{86}F, ^{88}L
^{164}R	^{358}G	
^{165}R	PO_4, ^{354}R	^{86}F
^{166}A	^{85}M	
^{167}S		
^{168}L		^{307}L, ^{308}Y
^{169}T		

*Sl*JAZ5	*Sl*COI1	
	H-Bond	Hydrophobic
^{328}V		
^{329}P		^{360}D
^{330}Q	^{357}R, ^{418}L ^{420}E	
^{331}A	JA-Ile	^{86}F
^{332}R	^{357}R	^{357}R
^{333}K	PO_4	^{85}M
^{334}A	^{85}M	^{170}E
^{335}S	^{170}E	^{198}M
^{336}L		^{307}L, ^{308}Y, ^{356}E
^{337}A		

654

655

656 **Figure 7.** *In silico* analyses of *At*COI1-JA-Ile-*At*JAZ1 (PDB ID: 3OGL, a, d, g), *Sl*COI1-
657 JA-Ile-*Sl*JAZ1 (b, e, h), and *Sl*COI1-JA-Ile --*Sl*JAZ5 (c, f, i) to show the binding mode
658 of the extended degron. (a-c) The amino acid residues forming hydrogen bonds (H-bond)
659 or hydrophobic interaction (Hydrophobic) between COI1 and JAZ observed in the crystal

structure of *At*COI1-JA-Ile-*At*JAZ1 (3OGL, a), MD simulation of *Sl*COI1-JA-Ile-*Sl*JAZ1 (b) and MD simulation of *Sl*COI1-JA-Ile-*Sl*JAZ5 (c). (d) The reported structure around the degron sequence of *At*JAZ1 in the complex of *At*COI1-JA-Ile-*At*JAZ1. (e, f) The obtained MD structure around the degron sequence of *Sl*JAZ in the complex of *Sl*COI1-JA-Ile-*Sl*JAZ1 (e) or *Sl*COI1-JA-Ile-*Sl*JAZ5 (f). (g) The reported structure around the DOD sequence of *At*JAZ1 in the complex of *At*COI1-JA-Ile-*At*JAZ1. (h, i) The obtained MD structure around the DOD sequence of *Sl*JAZ in the complex of *Sl*COI1-JA-Ile-*Sl*JAZ1 (h) or *Sl*COI1-JA-Ile-*Sl*JAZ5 (i).

669 **Table 1.** K_d values calculated from AlphaScreen analyses

*Sl*COI1-*Sl*JAZ	K_d / nM	
	JA-Ile	COR
*Sl*JAZ1	9.2	4.9
*Sl*JAZ2	134	12.1
*Sl*JAZ3	136	19.3
*Sl*JAZ4	1776	130
*Sl*JAZ5	4.2	0.64
*Sl*JAZ6	4.1	0.76
*Sl*JAZ7	16.2	0.23
*Sl*JAZ8	2.2	0.39
*Sl*JAZ9	1107	44.7
*Sl*JAZ10	402	89.7
*Sl*JAZ11	430	62.4
*Sl*JAZ13	637	80.7

670

Figures

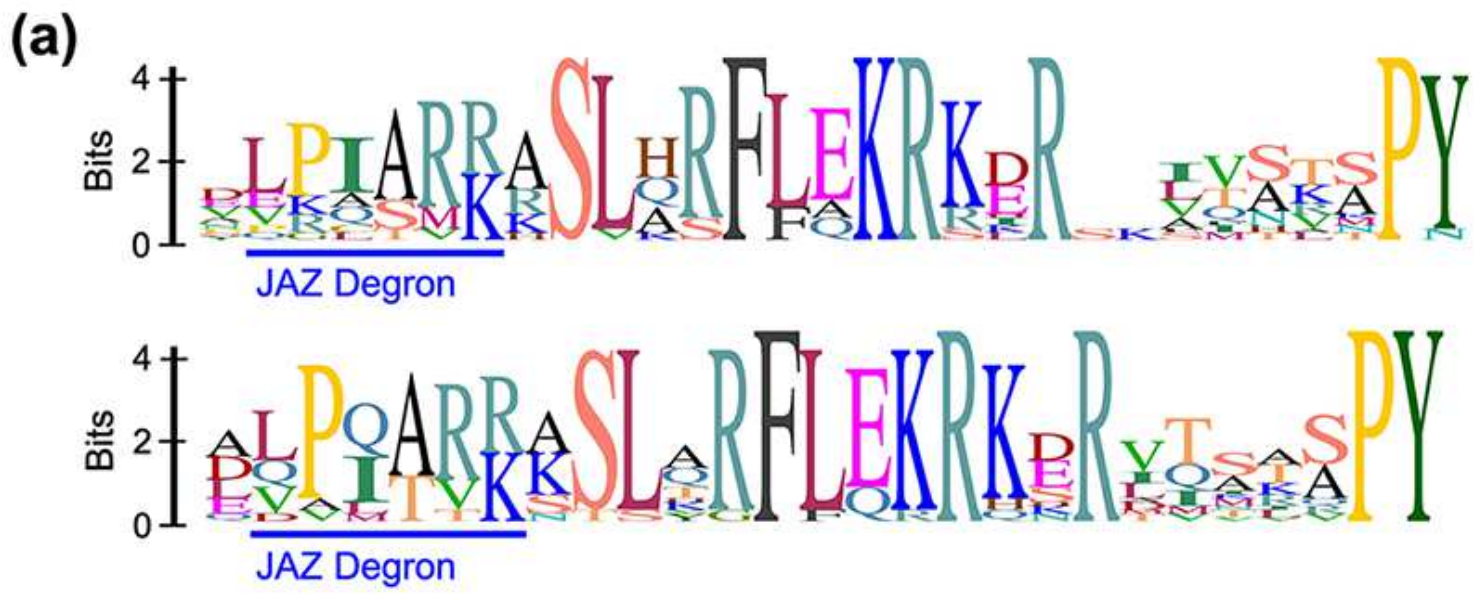

(b)

*At*JAZ1:	^{201}L	P	I	A	R	R
*At*JAZ2:	^{203}L	P	I	A	R	R
*At*JAZ3:	^{301}L	P	L	A	R	K
*At*JAZ4:	^{228}L	P	Q	T	R	K
*At*JAZ5:	^{180}E	R	I	A	R	R
*At*JAZ6:	^{184}E	R	I	A	R	R
*At*JAZ7:	^{119}Q	K	A	S	M	K
*At*JAZ8:	^{102}P	K	A	S	M	K
*At*JAZ9:	^{219}V	P	Q	A	R	K
*At*JAZ10:	^{167}L	P	I	A	R	R
*At*JAZ11:	^{196}V	P	I	A	R	R
*At*JAZ12:	^{138}L	P	I	A	R	R
*At*JAZ13:	^{83}L	G	C	S	V	K

*Sl*JAZ1:	^{160}L	P	I	A	R	R
*Sl*JAZ2:	^{197}L	P	I	A	R	R
*Sl*JAZ3:	^{250}L	P	I	A	R	R
*Sl*JAZ4:	^{154}L	P	I	A	R	R
*Sl*JAZ5:	^{328}V	P	Q	A	R	K
*Sl*JAZ6:	^{281}V	P	Q	A	R	K
*Sl*JAZ7:	^{174}L	A	M	A	R	R
*Sl*JAZ8:	^{193}V	P	Q	A	R	K
*Sl*JAZ9:	^{85}Q	P	Q	T	V	K
*Sl*JAZ10:	^{76}Q	P	Q	T	V	K
*Sl*JAZ11:	^{112}Q	P	Q	T	V	K
*Sl*JAZ12:	^{86}D	V	L	T	T	R
*Sl*JAZ13:	^{338}L	P	I	A	R	R

Figure 1

(a) Sequence logos of the Jas motif of AtJAZs (top) or SlJAZs (bottom). (b) The canonical JAZ degron sequences of AtJAZs (left) and SlJAZs (right).

Figure 2

(a) Pull down assay of GST-SlCOI1 with FLAG-SlJAZ (full-length proteins) in the presence of JA-Ile (100 nM). GST-SlCOI1 bound to FLAG-SlJAZ proteins was pulled down with anti-FLAG antibody and Protein G magnetic beads, and analyzed by immunoblotting (top: anti-GST-HRP conjugate for detection of GST-SlCOI1, bottom: anti-FLAG antibody and anti mouse-IgG HRP conjugate for detection of FLAG-SlJAZs). * or ** show the bands derived from heavy chain or light chain of the anti-FLAG antibody. (b) Pull down assay of GST-SlCOI1 with Fl-SlJAZPs in the presence of JA-Ile (100 nM). GST-SlCOI1 bound to Fl-SlJAZPs was pulled down with anti-fluorescein antibody and Protein G magnetic beads, and analyzed by immunoblotting (anti-GST-HRP conjugate for detection of GST-SlCOI1).

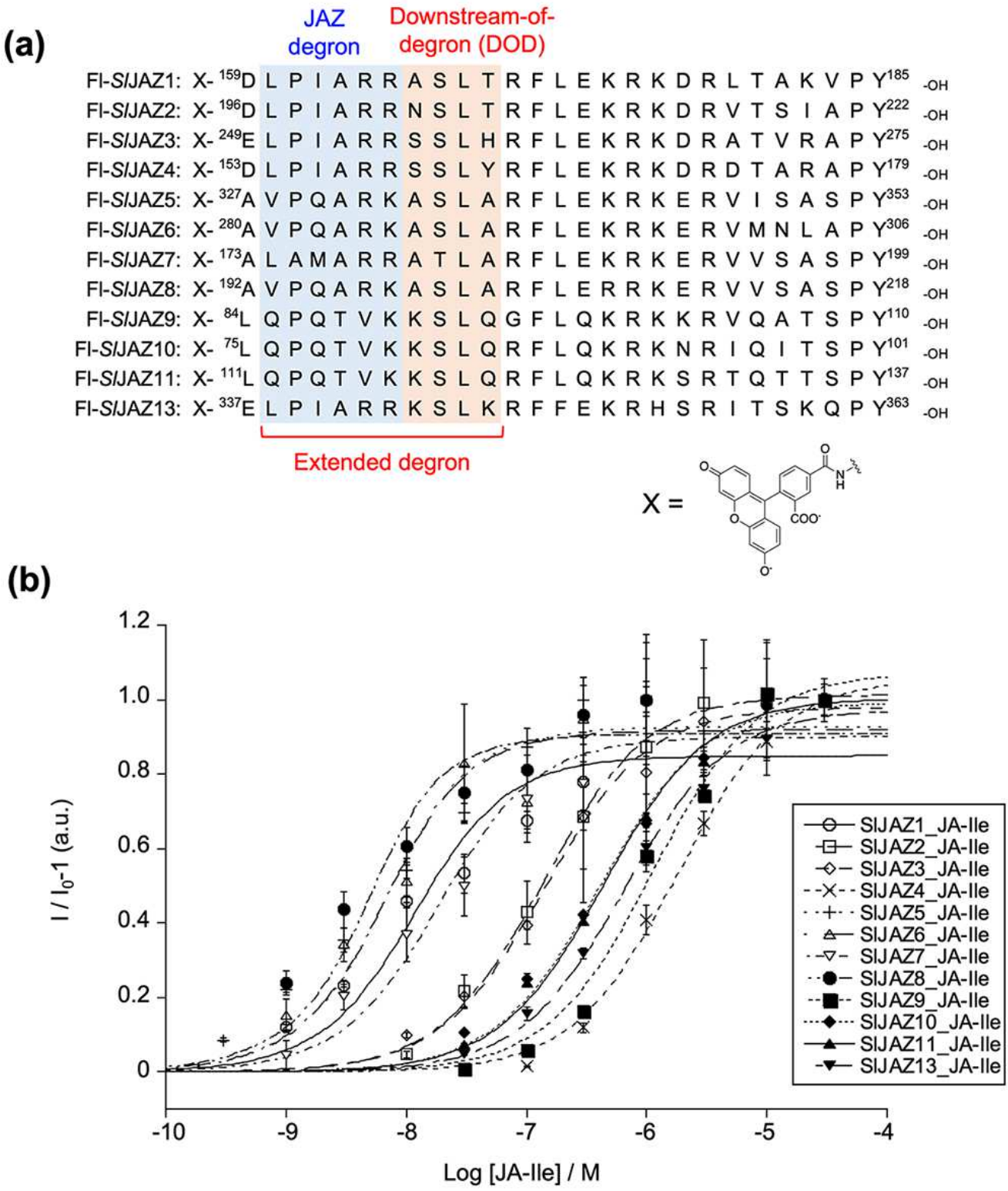

Figure 3

(a) Chemical structures of fluorescein-tagged SlJAZ1-11/13 degron short peptides (SlJAZP1-11/13). The canonical JAZ degron sequences were shown in blue frame and down-stream-of-degron (DOD) sequence were in orange frame. (b) AlphaScreen assays using Fl-SlJAZPs and GST-SlCOI1 with JA-Ile (0 – 30 μM). Experiments were performed in triplicate to obtain mean and S.D. (shown as error bars).

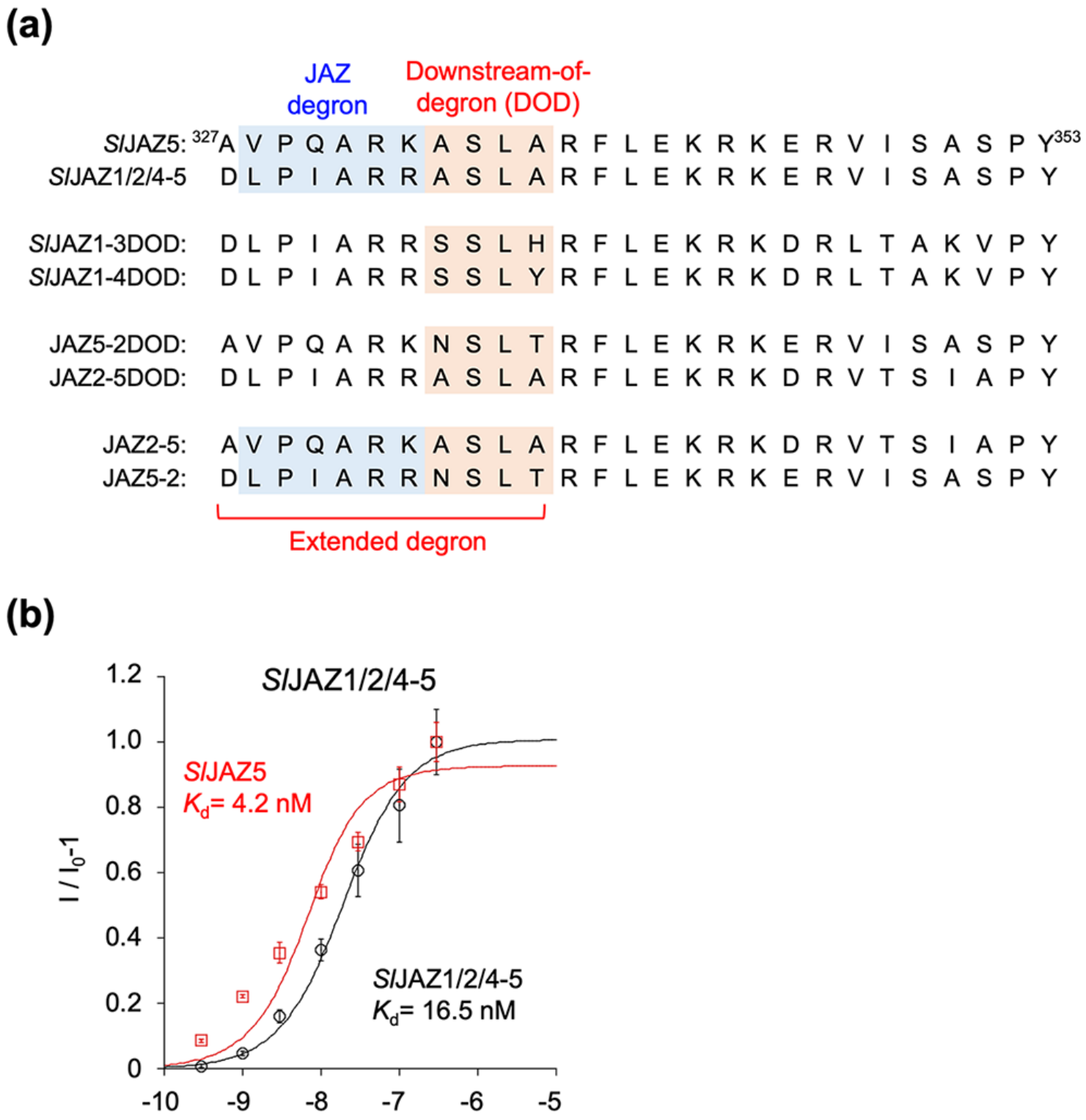

Figure 4

(a) Design of the swapped SlJAZ peptides (SlJAZ5, 1/2/4-5, 1-3DOD, 1-4DOD 5-2DOD, 2-5DOD, 2-5, 5-2). The canonical JAZ degron sequences were shown in blue frame and down-stream-of-degron (DOD) sequence were in orange frame. (b) AlphaScreen assay using GST-SlCOI1 and Fl-SlJAZP1/2/4-5 (black circle) or Fl-SlJAZ5 (red square) with JA-Ile (0 – 300 nM). Experiments were performed in triplicate to obtain mean and S.D. (shown as error bars).

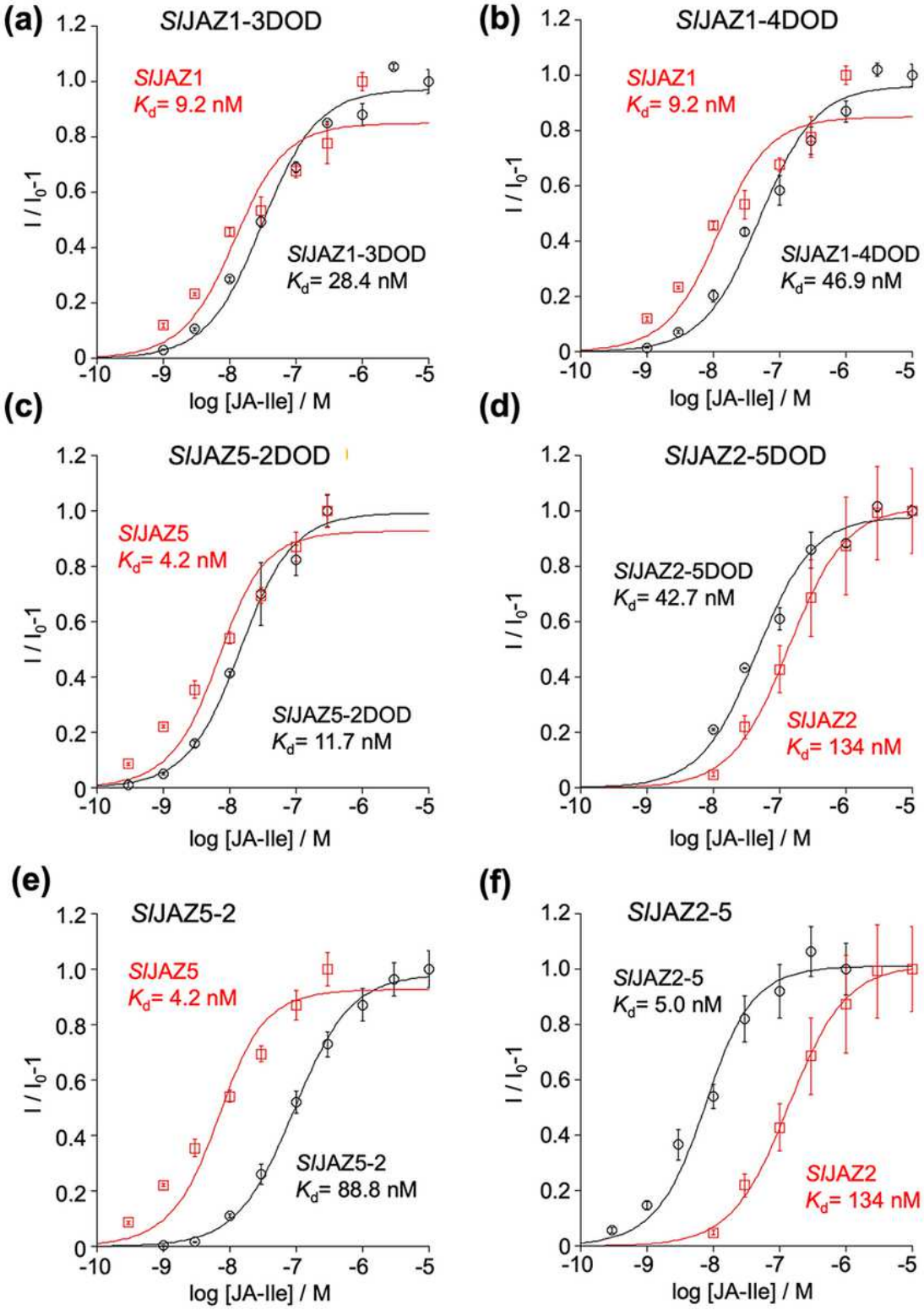

Figure 5

Alphascreen assay of swapped Fl-SlJAZPs (a: SlJAZ1-3DOD, b: 1-4DOD, c: 5-2DOD, d: 2-5DOD, e: 5-2, f: 2-5) to consider the extended degron sequence. Signal intensity change of AlphaScreen of swapped Fl-SlJAZPs 640 and GST-SlCOI1 upon addition of JA-Ile (0-10 μM). Black circles show the results of swapped SlJAZPs and red squares show those of corresponding natural SlJAZPs, respectively. Experiments were performed in triplicate to obtain mean and S.D. (shown as error bars).

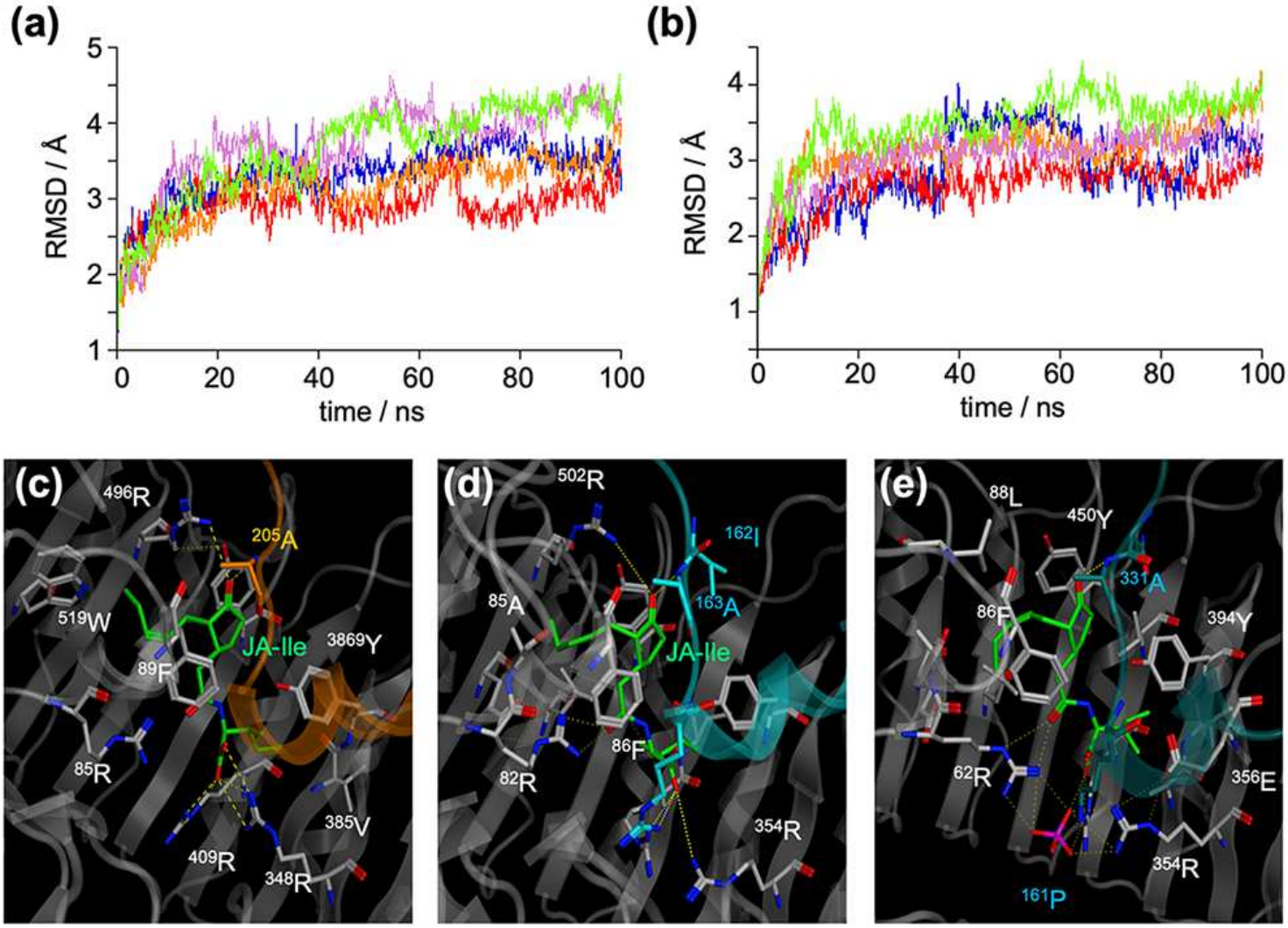

Figure 6

(a, b) The RMSDs of backbone atoms of the complex of SlCOI1-JA-Ile-SlJAZ1 (a) and SlCOI1-JA-Ile-SlJAZ5 (b) as a function of MD time step. (c) The reported 649 structure of the ligand binding pocket of AtCOI1-JA-Ile-AtJAZ1 (PDB ID: 3OGL). (d, e) The representative structure of the ligand binding pocket of SlCOI1-JA-Ile-SlJAZ1 (d) and that of SlCOI1-JA-Ile-SlJAZ5 (e), which was obtained by homology modeling and MD simulation.

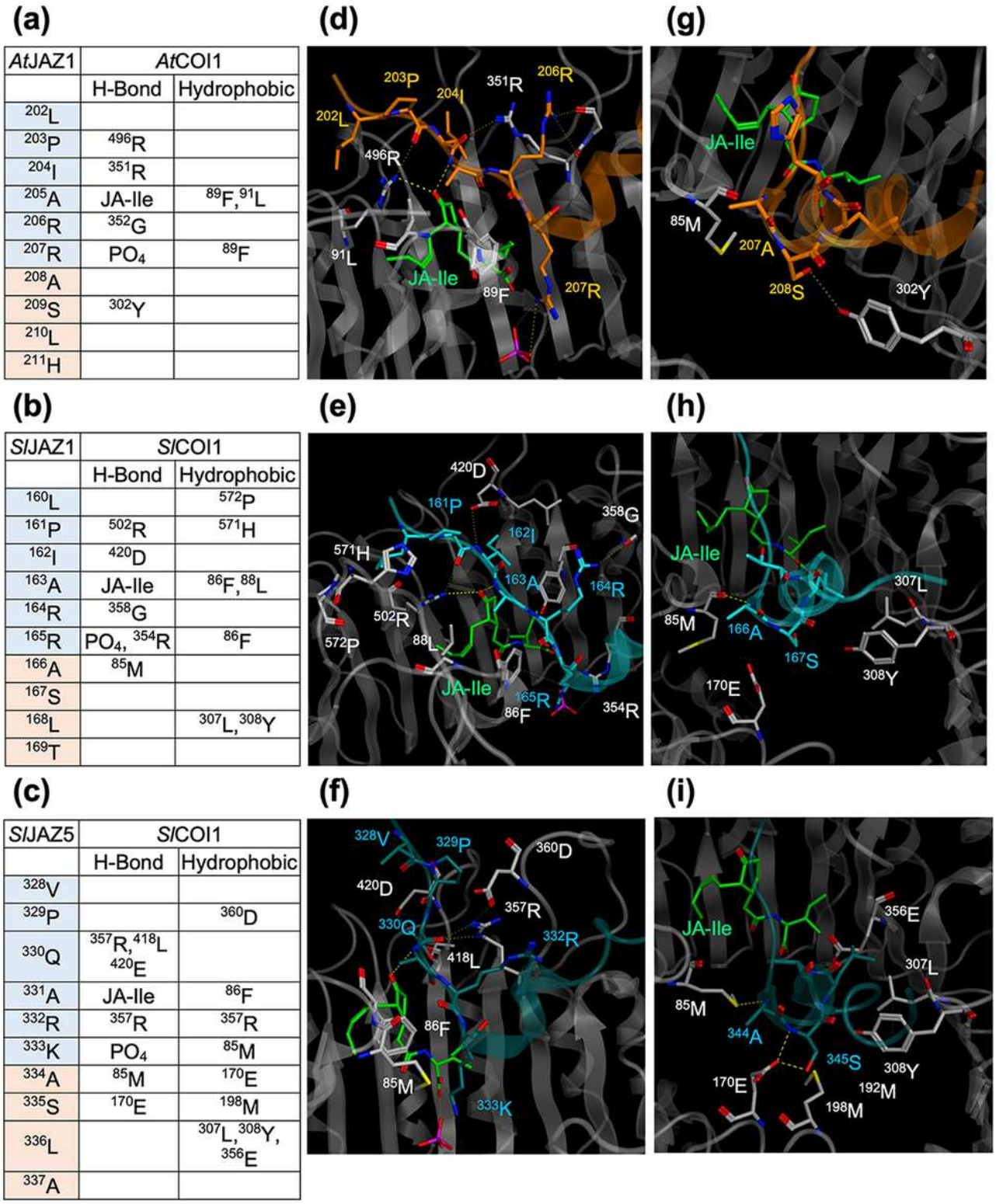

Figure 7

In silico analyses of AtCOI1-JA-Ile-AtJAZ1 (PDB ID: 3OGL, a, d, g), SlCOI1- JA-Ile-SlJAZ1 (b, e, h), and SlCOI1-JA-Ile –SlJAZ5 (c, f, i) to show the binding mode of the extended degron. (a-c) The amino acid residues forming hydrogen bonds (H-bond) or hydrophobic interaction (Hydrophobic) between COI1 and JAZ observed in the crystal structure of AtCOI1-JA-Ile-AtJAZ1 (3OGL, a), MD simulation 660 of SlCOI1-JA-Ile-SlJAZ1 (b) and MD simulation of SlCOI1-JA-Ile-SlJAZ5 (c). (d) The reported structure around the

degron sequence of AtJAZ1 in the complex of AtCOI1-JA-Ile-AtJAZ1. (e, f) The obtained MD structure around the degron sequence of SlJAZ in the complex of SlCOI1- JA-Ile-SlJAZ1 (e) or SlCOI1-JA-Ile-SlJAZ5 (f). (g) The reported structure around the DOD sequence of AtJAZ1 in the complex of AtCOI1-JA-Ile-AtJAZ1. (h, i) The obtained MD structure around the DOD sequence of SlJAZ in the complex of SlCOI1-JA-Ile- SlJAZ1 (h) or SlCOI1-JA-Ile-SlJAZ5 (i).